Chapter 8

# Overvoltages, testing procedures and insulation coordination

Power systems are always subjected to overvoltages that have their origin in atmospheric discharges in which case they are called external or lightning overvoltages, or they are generated internally by connecting or disconnecting the system, or due to the systems fault initiation or extinction. The latter type are called internal overvoltages. This class may be further subdivided into (i) temporary overvoltages, if they are oscillatory of power frequency or harmonics, and (ii) switching overvoltages, if they are heavily damped and of short duration. Temporary overvoltages occur almost without exception under no load or very light load conditions. Because of their common origin the temporary and switching overvoltages occur together and their combined effect has to be taken into account in the design of h.v. systems insulation.

The magnitude of the external or lightning overvoltages remains essentially independent of the system's design, whereas that of internal or switching overvoltages increases with increasing the operating voltage of the system. Hence, with increasing the system's operating voltage a point is reached when the switching overvoltages become the dominant factor in designing the system's insulation. Up to approximately 300 kV, the system's insulation has to be designed to withstand primarily lightning surges. Above that voltage, both lightning and switching surges have to be considered. For ultra-h.v. systems, 765 kV and above switching overvoltages in combination with insulator contamination become the predominating factor in the insulation design.[1]* For the study of overvoltages occurring in power systems, a thorough knowledge of surge propagation laws is needed which can be found in a number of textbooks[2,3] and will not be discussed here.

## 8.1 The lightning mechanism

Physical manifestations of lightning have been noted in ancient times, but the understanding of lightning is relatively recent. Franklin carried out experiments on lightning in 1744–1750, but most of the knowledge has been obtained over the last 50 to 70 years. The real incentive to study lightning came when electric transmission lines had to be protected against lightning. The methods

include measurements of (i) lightning currents, (ii) magnetic and electromagnetic radiated fields, (iii) voltages, (iv) use of high-speed photography and radar.

Fundamentally, lightning is a manifestation of a very large electric discharge and spark. Several theories have been advanced to explain accumulation of electricity in clouds and are discussed in references 4, 5 and 6. The present section reviews briefly the lightning discharge processes.

In an active thunder cloud the larger particles usually possess negative charge and the smaller carriers are positive. Thus the base of a thunder cloud generally carries a negative charge and the upper part is positive, with the whole being electrically neutral. The physical mechanism of charge separation is still a topic of research and will not be treated here. As will be discussed later, there may be several charge centres within a single cloud. Typically the negative charge centre may be located anywhere between 500 m and 10 000 m above ground. Lightning discharge to earth is usually initiated at the fringe of a negative charge centre.

To the eye a lightning discharge appears as a single luminous discharge, although at times branches of variable intensity may be observed which terminate in mid-air, while the luminous main channel continues in a zig-zag path to earth. High-speed photographic technique studies reveal that most lightning strokes are followed by repeat or multiple strokes which travel along the path established by the first stroke. The latter ones are not usually branched and their path is brightly illuminated.

The various development stages of a lightning stroke from cloud to earth as observed by high-speed photography is shown diagrammatically in Fig. 8.1

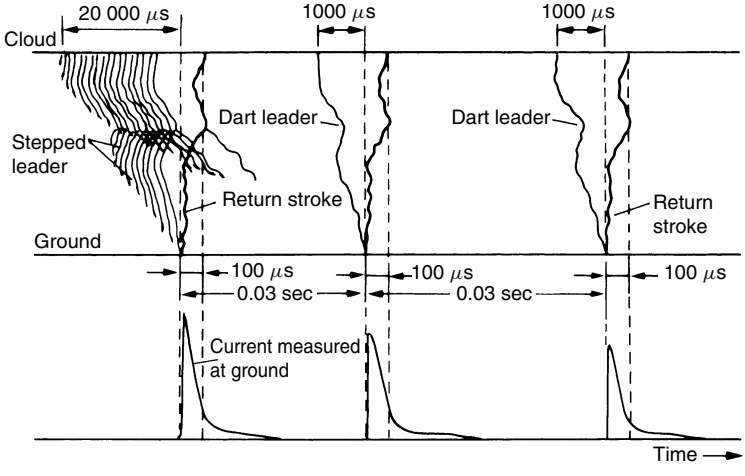


**Figure 8.1** *Diagrammatic representation of lightning mechanism and ground current*[3]

together with the current to ground. The stroke is initiated in the region of the negative charge centre where the local field intensity approaches ionization field intensity ($\cong$30 kV/cm in atmospheric air, or $\sim$10 kV/cm in the presence of water droplets).

During the first stage the leader discharge, known as the 'stepped leader', moves rapidly downwards in steps of 50 m to 100 m, and pauses after each step for a few tens of microseconds. From the tip of the discharge a 'pilot streamer' having low luminosity and current of a few amperes propagates into the virgin air with a velocity of about $1 \times 10^5$ m/sec. The pilot streamer is followed by the stepped leader with an average velocity of about $5 \times 10^5$ m/sec and a current of some 100 A. For a stepped leader from a cloud some 3 km above ground shown in Fig. 8.1 it takes about 60 m/sec to reach the ground. As the leader approaches ground, the electric field between the leader and earth increases and causes point discharges from earth objects such as tall buildings, trees, etc. At some point the charge concentration at the earthed object is high enough to initiate an upwards positive streamer. At the instance when the two leaders meet, the 'main' or 'return' stroke starts from ground to cloud, travelling much faster ($\sim 50 \times 10^6$ m/sec) along the previously established ionized channel. The current in the return stroke is in the order of a few kA to 250 kA and the temperatures within the channel are 15 000°C to 20 000°C and are responsible for the destructive effects of lightning giving high luminosity and causing explosive air expansion. The return stroke causes the destructive effects generally associated with lightning.

The return stroke is followed by several strokes at 10- to 300-m/sec intervals. The leader of the second and subsequent strokes is known as the 'dart leader' because of its dart-like appearance. The dart leader follows the path of the first stepped leader with a velocity about 10 times faster than the stepped leader. The path is usually not branched and is brightly illuminated.

A diagrammatic representation of the various stages of the lightning stroke development from cloud to ground in Figs 8.2(a) to (f) gives a clearer appreciation of the process involved. In a cloud several charge centres of high concentration may exist. In the present case only two negative charge centres are shown. In (a) the stepped leader has been initiated and the pilot streamer and stepped leader propagate to ground, lowering the negative charges in the cloud. At this instance the striking point still has not been decided; in (b) the pilot streamer is about to make contact with the upwards positive streamer from earth; in (c) the stroke is completed, a heavy return stroke returns to cloud and the negative charge of cloud begins to discharge; in (d) the first centre is completely discharged and streamers begin developing in the second charge centre; in (e) the second charge centre is discharging to ground via the first charge centre and dart leader, distributing negative charge along the channel. Positive streamers are rising up from ground to meet the dart leader;

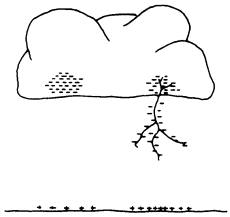

(a) Charge centres in cloud; pilot streamer and stepped leader propagate earthward; outward branching of streamers to earth. Lowering of charge into space beneath cloud.

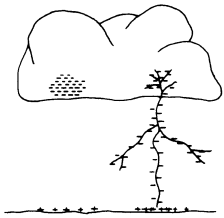

(b) Process of (a) almost completed; pilot streamer about to strike earth.

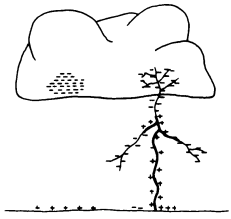

(c) Heavy return streamer; discharge to earth of negatively charged space beneath cloud.

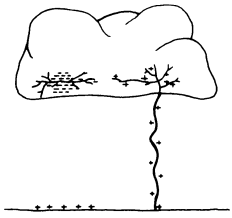

(d) First charge centre completely discharged; development of streamers between charge centres within cloud.

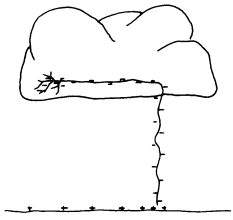

(e) Discharge between two charge centres; dart leader propagates to ground along original channel; dart leader about to strike earth; negative charge lowered and distributed along stroke channel.

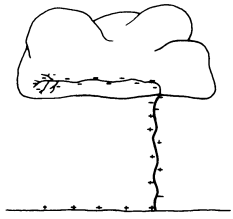

(f) Heavy return streamer discharge to earth of negatively charged space beneath cloud.

**Figure 8.2** *Schematic representation of various stages of lightning stroke between cloud and ground*[6]

(f) contact is made with streamers from earth, heavy return stroke proceeds upwards and begins to discharge negatively charged space beneath the cloud and the second charge centre in the cloud.

Lightning strokes from cloud to ground account only for about 10 per cent of lightning discharges, the majority of discharges during thunderstorms

take place between clouds. Discharges within clouds often provide general illumination known as 'sheath lightning'.

Measurements of stroke currents at ground have shown that the high current is characterized by a fast rise to crest (1 to 10 μsec) followed by a longer decay time of 50–1000 μsec to half-time. Figure 8.3 gives the probability distribution of times to crest for lightning strokes as prepared by Anderson.[7] There is evidence that very high stroke currents do not coincide with very short times to crest. Field data[3,20] indicate that 50 per cent of stroke currents including multiple strokes have a rate of rise exceeding 20 kA/μsec and 10 per cent exceed 50 kA/μsec. The mean duration of stroke currents above half value is 30 μsec and 18 per cent have longer half-times than 50 μsec. Thus for a typical maximum stroke current of 10 000 A a transmission line of surge impedance (say) $Z = 400\,\Omega$ and assuming the strike takes place in the middle of the line with half of the current flowing in each direction ($Z \cong 200\,\Omega$) the lightning overvoltage becomes $V = 5000 \times 400 = 2\,\text{MV}$. Based on many investigations the AIEE Committee[8] has produced the frequency distribution of current magnitudes, shown in Fig. 8.4, which is often used for performance calculations. Included in Fig. 8.4 is a curve proposed by Anderson.[7]

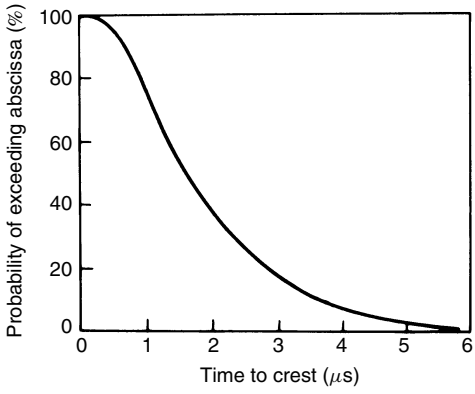


**Figure 8.3** *Distribution of times to crest of lightning stroke currents (after Anderson*[7]*)*

The data on lightning strokes and voltages has formed the basis for establishing the standard impulse or lightning surge for testing equipment in laboratories. The standard lightning impulse waveshape will be discussed later in this chapter.

### *8.1.1 Energy in lightning*

To estimate the amount of energy in a typical lightning discharge let us assume a value of potential difference of $10^7$ V for a breakdown between a cloud

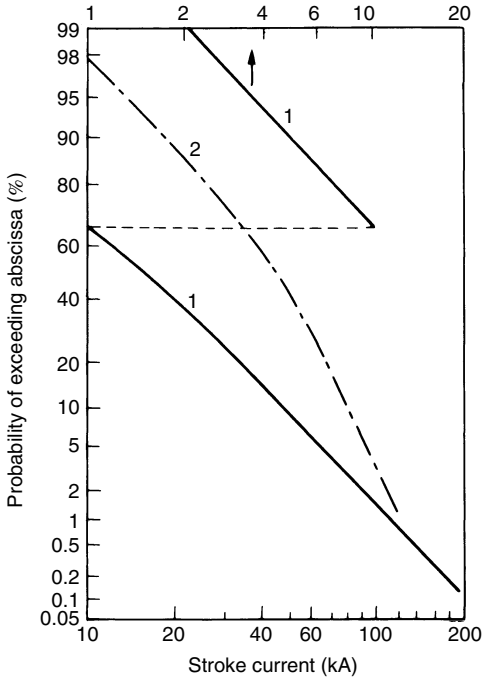


**Figure 8.4** *Cumulative distributions of lightning stroke current magnitudes: 1. After AIEE Committee.*[8] *2. After Anderson*[6]

and ground and a total charge of 20 coulombs. Then the energy released is $20 \times 10^7$ Ws or about 55 kWh in one or more strokes that make the discharge. The energy of the discharge dissipated in the air channel is expended in several processes. Small amounts of this energy are used in ionization of molecules, excitations, radiation, etc. Most of the energy is consumed in the sudden expansion of the air channel. Some fraction of the total causes heating of the struck earthed objects. In general, lightning processes return to the global system the energy that was used originally to create the charged cloud.

### *8.1.2 Nature of danger*

The degree of hazard depends on circumstances. To minimize the chances of being struck by lightning during thunderstorm, one should be sufficiently far away from tall objects likely to be struck, remain inside buildings or be well insulated.

A direct hit on a human or animal is rare; they are more at risk from indirect striking, usually: (a) when the subject is close to a parallel hit or other tall object, (b) due to an intense electric field from a stroke which can

induce sufficient current to cause death, and (c) when lightning terminating on earth sets up high potential gradients over the ground surface in an outwards direction from the point or object struck. Figure 8.5 illustrates qualitatively the current distribution in the ground and the voltage distribution along the ground extending outwards from the edge of a building struck by lightning.[9] The potential difference between the person's feet will be largest if his feet are separated along a radial line from the source of voltage and will be negligible if he moves at a right angle to such a radial line. In the latter case the person would be safe due to element of chance.

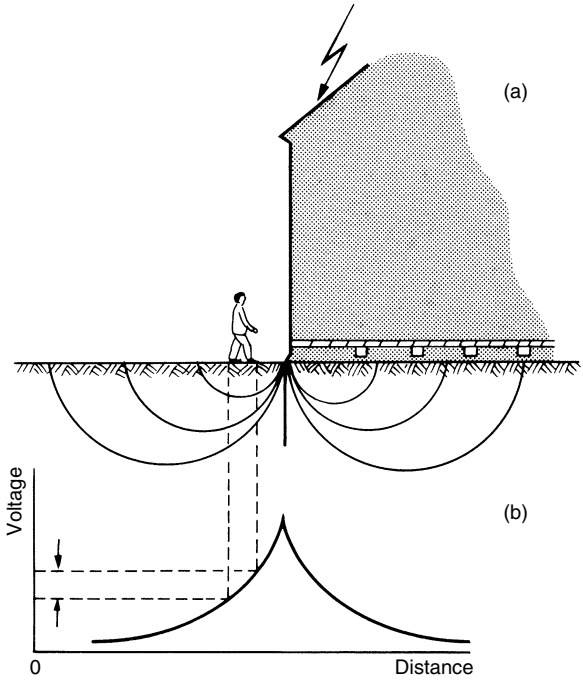


**Figure 8.5** *Current distribution and voltage distribution in ground due to lightning stroke to a building (after Golde[9])*

## 8.2 Simulated lightning surges for testing

The danger to electric systems and apparatus comes from the potentials that lightning may produce across insulation. Insulation of power systems may be classified into two broad categories: external and internal insulation. External insulation is comprised of air and/or porcelain, etc., such as conductor-to-tower clearances of transmission lines or bus supports. If the potential caused

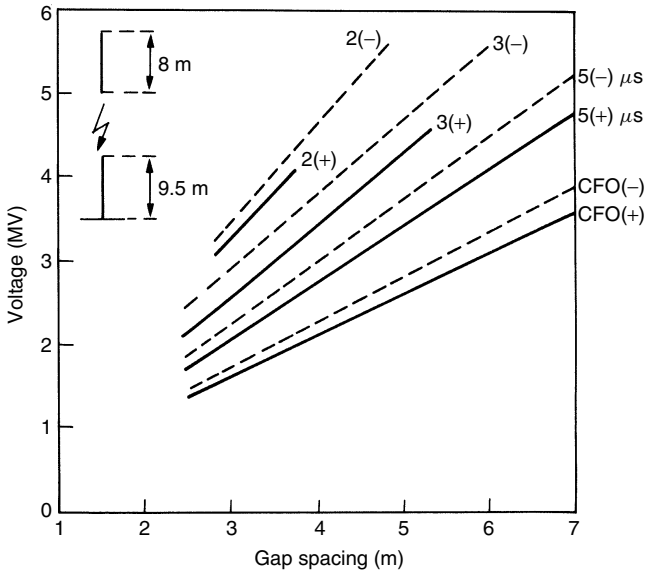


**Figure 8.6** *Impulse (1.2/50 μsec) flashover characteristics of long rod gaps corrected to STP (after Udo[10])*

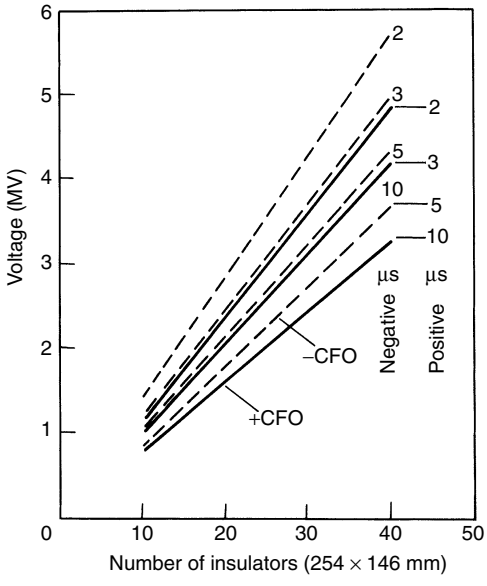


**Figure 8.7** *Impulse (1.2/50 μsec) flashover characteristics for long insulator strings (after Udo[10])*

by lightning exceeds the strength of insulation, a flashover or puncture occurs. Flashover of external insulation generally does not cause damage to equipment. The insulation is 'self-restoring'. At the worst a relatively short outage follows to allow replacement of a cheap string of damaged insulation. Internal insulation most frequently consists of paper, oil or other synthetic insulation which insulates h.v. conductors from ground in expensive equipment such as transformers, generators, reactors, capacitors, circuit-breakers, etc. Failure of internal insulation causes much longer outages. If power arc follows damage to equipment it may be disastrous and lead to very costly replacements.

The system's insulation has to be designed to withstand lightning voltages and be tested in laboratories prior to commissioning.

Exhaustive measurements of lightning currents and voltages and long experience have formed the basis for establishing and accepting what is known as the standard surge or 'impulse' voltage to simulate external or lightning overvoltages. The international standard lightning impulse voltage waveshape is an aperiodic voltage impulse that does not cross the zero line which reaches its peak in 1.2 μsec and then decreases slowly (in 50 μsec) to half the peak value. The characteristics of a standard impulse are its polarity, its peak value, its front time and its half value time. These have been defined in Chapter 2, Fig. 2.23.

Extensive laboratory tests have shown that for external insulation the lightning surge flashover voltages are substantially proportional to gap length and that positive impulses give significantly lower flashover values than negative ones. In addition, for a particular test arrangement, as the applied impulse crest is increased the instant of flashover moves from the tail of the wave to the crest and ultimately to the front of the wave giving an impulse voltage–time ('$V-T$') characteristic as was discussed in Chapter 5, Fig. 5.45. Figures 8.6 and 8.7 show typical impulse sparkover characteristics for long rod gaps and suspension insulators obtained by Udo[10] at various times to flashover. These figures include the critical or long time flashover characteristics (CFO) occurring at about 10 μsec on the wave tail as well as the characteristics corresponding to shorter time lags near the wave crest. Data for both polarities are shown. The values plotted in Figs 8.6 and 8.7 have been corrected to standard atmospheric conditions.

## 8.3 Switching surge test voltage characteristics

In power transmission systems with systems voltages of 245 kV and above, the electrical strength of the insulation to switching overvoltages becomes important for the insulation design. A considerable amount of data on breakdown under switching surges is available. However, a variety of switching surge waveshapes and the correspondingly large range of flashover values

make it difficult to choose a standard shape of switching impulses. Many tests have shown that the flashover voltage for various geometrical arrangements under unidirectional switching surge voltages decreases with increasing the front duration of the surge, reaching the lowest value somewhere in the range between 100 and 500 μsec. The time to half-value has less effect upon the breakdown strength because flashover almost always takes place before or at the crest of the wave. Figure 8.8 illustrates a typical relationship for a critical flashover voltage per metre as a function of time to flashover for a 3-m rod-rod gap and a conductor-plane gap respectively.[11] It is seen that the standard impulse voltages give the highest flashover values, with the switching surge values of crest between approx. 100 and 500 μsec falling well below the corresponding power frequency flashover values.

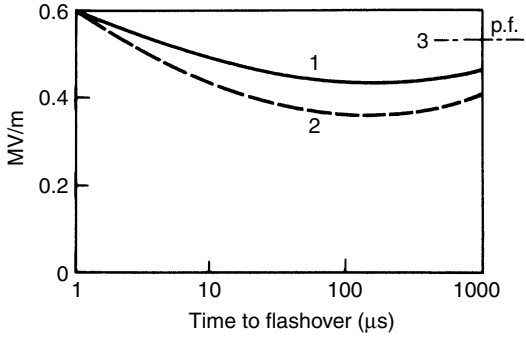


**Figure 8.8** *Relationship between vertical flashover voltage per metre and time to flashover (3 m gap). 1. Rod-rod gap. 2. Conductor-plane gap. 3. Power frequency*

The relative effect of time to crest upon flashover value varies also with the gap spacing and humidity.[21] Figure 8.9 compares the positive flashover characteristics of standard impulses and 200/2000 μsec with power frequency voltages for a rod-rod gap plotted as flashover voltage per metre against gap spacing.[11] We observe a rapid fall in switching surge breakdown strength with increasing the gap length. This drastic fall in the average switching surge strength with increasing the insulation length leads to costly design clearances, especially in the ultra-h.v. regions. All investigations show that for nearly all gap configurations which are of practical interest, positive switching impulses result in lower flashover voltage than negative ones. The flashover behaviour of external insulations with different configurations under positive switching impulse stress is therefore most important. The switching surge voltage breakdown is also affected by the air humidity. Kuffel *et al.*[22] have reported that over the range from 3 to 16 g/m$^3$ absolute humidity, the breakdown voltage

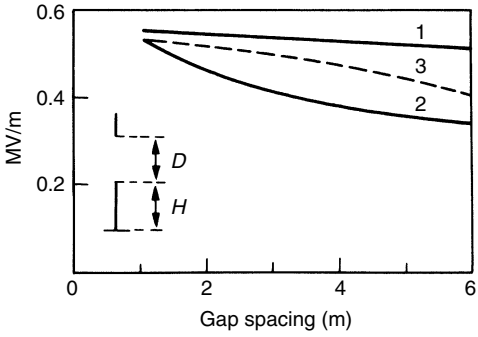


**Figure 8.9** *Relationship between flashover voltage (MV/m) and gap length for 1: 1.2/50 μsec impulses, 2: 200/2000 μsec switching surges and 3: power frequency voltages*

of positive rod gaps increases approximately 1.7 per cent per 1 g/m$^3$ increase in absolute humidity.

For testing purposes the standard switching surge recommended by IEEE St-4-1995 Publication[12] and IEC Publication 60-1[13] 1998-11 has a front time $T_2 = 2500\,\mu\text{sec} \pm 20$ per cent and half-time value $T_2 = 2500\,\mu\text{sec} \pm 60$ per cent. The general designation for a standard switching impulse is given as 250/2500 μsec. The front is counted from the actual beginning of the impulse till the peak value is reached. Full characteristics of a standard switching test surge have been defined in Chapter 2, Fig. 2.24.

It was shown in Chapter 5, section 5.9 that in non-uniform field gaps the shape of both electrodes affects the formation and propagation of streamers and directly influences the flashover values. This explains the different flashover values observed for various insulating structures, especially under switching surges. Much of the laboratory flashover data for large gaps under switching surges have been obtained for rod-plane gaps. Subsequently, several attempts have been made to relate data for other structures to rod-plane gap data. Several investigators[14,15] have shown that the positive 50 per cent switching surge voltage of different structures in air in the range from 2 to 8 m follow the expression

$$V_{50} = k\,500\,d^{0.6}\ \text{kV} \tag{8.1}$$

where $d$ is the gap length in metres and $k$ is gap factor relating to the electrodes geometry. For rod-plane gaps the factor $k$ is accepted as unity. Thus, the 'gap factor' $k$ represents a proportionality factor of the 50 per cent flashover voltage of any gap geometry to that of a rod-plane gap for the same distance or

$$k = \frac{V_{50}}{V_{50}\ \text{rod-plane}} \tag{8.2}$$

Expression (8.1) applies to data obtained under the switching impulse of constant time to crest. A more general expression which gives minimum strength and applies to longer times to crest has been proposed by Gallet and Leroy[16] as follows:

$$V_{50} = \frac{k3450}{1 + \frac{8}{d}} \text{ kV} \tag{8.3}$$

where $k$ and $d$ have the same meaning as in expression (8.1).

In expression (8.2) only the function $V_{50}$ rod-plane is influenced by the switching impulse shape, while the gap factor $k$ depends only on the gap geometry and hence upon the field distribution in the gap. The parameters influencing the gap factor ($k$) have been fully discussed by Schneider and Weck.[17] These authors have measured the gap factor ($k$) for different gap geometries and spacings using a large three-dimensional electrolytic tank and modelling scaled down gaps. Their data are included in Table 8.1. The corresponding geometric configurations are shown in Fig. 8.10(a) to (f).

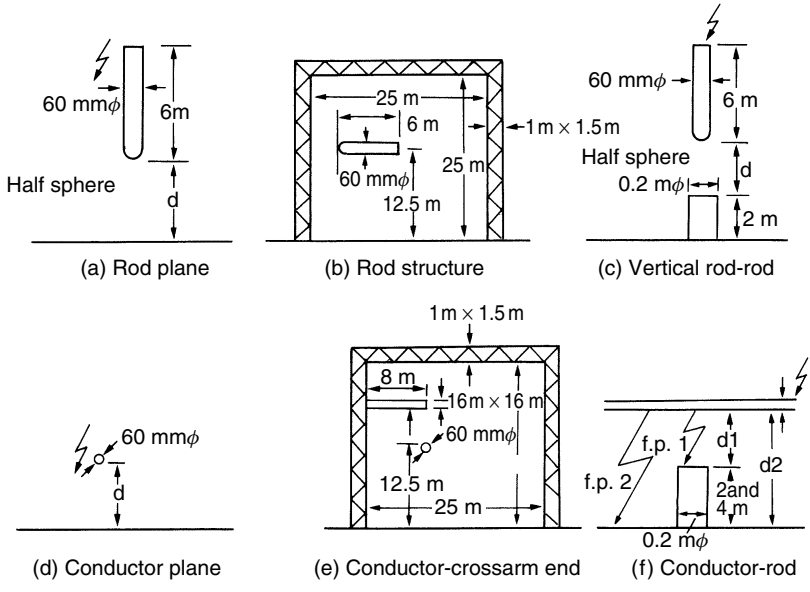


**Figure 8.10** *Configuration (gap factor)*

Expressions (8.1) and (8.3) together with data presented in Table 8.1 can be used in estimating required clearances in designing e.h.v. and u.h.v. structures. Refinements to these expressions are being introduced as more data become available.

**Table 8.1** *Geometric gap factor for various structures*

| *Configuration* | *Figure* | $d = 2\,m$ $k$ | $d = 3\,m$ $k$ | $d = 4\,m$ $k$ | $d = 6\,m$ $k$ |
|---|---|---|---|---|---|
| Rod-plane | (a) | 1 | 1 | 1 | 1 |
| Rod-structure | (b) | 1.08 | – | 1.07 | 1.06 |
| Rod-rod vertical $H = 2\,\text{m}$ | (c) | 1.27 | 1.26 | 1.21 | 1.14 |
| Conductor-plane | (d) | 1.08 | – | 1.14 | 1.15 |
| Conductor-cross arm end | (e) | 1.57 | 1.68 | 1.65 | 1.54 |
| Conductor-2m rod | (f) | 1.47 | – | 1.40 | 1.25 |
| Conductor-4m rod | (f) | 1.55 | – | 1.54 | 1.40 |

## 8.4 Laboratory high-voltage testing procedures and statistical treatment of results

Practical high voltage insulation systems comprise various types of dielectrics, e.g. gases, liquids, solids or any combination of these. The result, following the application of a voltage stress to insulation, individually and also collectively, is a discharge or withstand, and has a random nature. Hence the parameters characterizing the behaviour of the insulation must be handled statistically.

Test methods and procedures adopted for the determination of the parameters characterizing insulation behaviour generally involve the repeated application of dielectric stress and the appropriate evaluation of the results. The aim of the statistical evaluation of the test methods is to establish procedures for relevant interpretation of the parameters characterizing the insulation behaviour and to determine confidence limits for the data obtained. Hence a brief treatment of the statistical methods generally used will be presented.

The documents addressing this issue are the IEEE Standard[12] and the IEC Publication 60-1 1989-11.[13]

### *8.4.1 Dielectric stress–voltage stress*

A voltage stress when applied to a piece of insulation is completely defined when the applied voltage $V(t)$ is known during the time of stress ($t_O$, $t_M$). Trying to correlate the behaviour of the insulation to even a slightly different

value of $V(t)$ requires accurate knowledge of the physical processes occurring inside the insulation.

### 8.4.2 Insulation characteristics

The main characteristic of interest of an insulation is the disruptive discharge which may occur during the application of stress. However, because of the randomness of the physical processes which lead to disruptive discharge, the same stress applied several times in the same conditions may not always cause disruptive discharge. Also, the discharge when it occurs may occur at different times. In addition, the application of the stress, even if it does not cause discharge, may result in a change of the insulation characteristics.

### 8.4.3 Randomness of the appearance of discharge

Randomness of the appearance of discharge can be modelled by considering a large number of stress applications, a fraction $p$ of which causes discharge, $D$, and the remaining fraction $q = (1 - p)$ being labelled as withstand, $W$. The value of $p$ depends on applied stress, $S$, with $p = p(S)$ being the 'probability of discharge' and it represents one of the characteristics of the insulation. Recognizing that the time to discharge will also vary statistically, the probability of discharge will become a function of both the stress, $S$, and the time $t$.

$$p(V) = p(t, S) \tag{8.4}$$

### 8.4.4 Types of insulation

Insulations are grouped broadly into:

(i) Self-restoring (gases) – no change produced by the application of stress or by discharge, hence the same sample can be tested many times.
(ii) Non-self-restoring (liquids) – affected by discharge only, the same sample can be used until discharge occurs.
(iii) Affected by applied stress, insulation experiences ageing and in testing it becomes necessary to introduce a new parameter related to the sequential application of stress.

### 8.4.5 Types of stress used in high-voltage testing

For design purposes it is sufficient to limit the knowledge of the insulation characteristics to a few families of stresses which are a function of time $V(t)$ e.g. switching surge of double exponential with time to crest $T_1$ and to half

value $T_2$ and the variable crest value $V$ (see definitions in Chapter 2 for lightning and switching surges). For testing purposes, the family is further restricted by using fixed times $T_1$ and $T_2$, hence only one variable is left ($V$). The same applies to both types of surges. The behaviour of the insulation is then defined by the discharge probability as a function of crest voltage $p = p(V)$.

The most commonly used distribution function is the normal (Gaussian) distribution which has a particular shape (bell shape), plotted in Fig. 8.11. The equation for the normal distribution density function is

$$p(f) = \frac{1}{\sigma\sqrt{2\pi}} e^{-((f_k - f_{av})^2/2\sigma^2)} \tag{8.5}$$

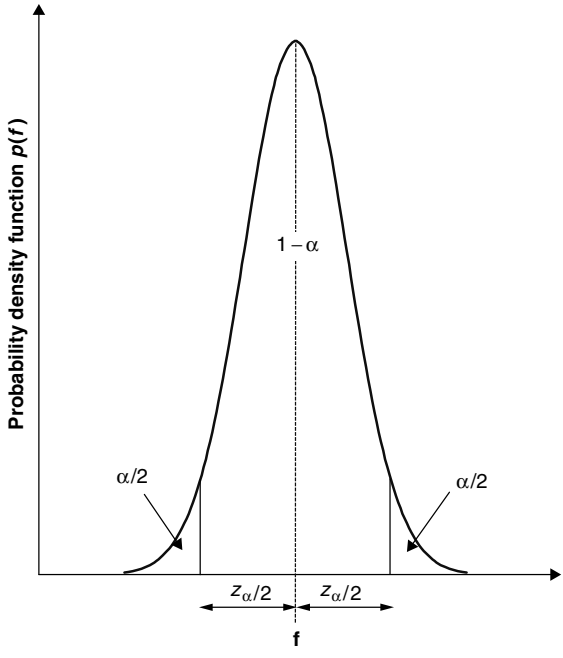


**Figure 8.11** *Gaussian (normal) distribution curve with confidence limits*

where $f_k$ is the $k_{\text{th}}$ value of the variable, $f_{\text{av}}$ is the average value and $\sigma$ is the standard deviation. When the applied voltage, $V$, becomes the variable the Gaussian distribution function used takes the form

$$p(V) = \frac{1}{\sigma\sqrt{2\pi}} e^{-((V - V_{50})^2/2\sigma^2)} \tag{8.6}$$

where $V_{50}$ is the voltage which leads to 50 per cent probability of discharge.

The knowledge of $V_{50}$ and $\sigma$ allows us to calculate the value of the probability $p(V)$ for any applied voltage.

Also shown In Fig. 8.11 are the confidence limits $A$ and $B$. The confidence in our results when expressed in per cent is shown by the area $(1 - \alpha)$ between the limits $-(\alpha/2)$ and $+(\alpha/2)$. A more convenient form of the normal distribution is the cumulative distribution function, the integral of eqn (8.12), which has the form

$$P(V) = \frac{1}{\sigma\sqrt{2\pi}} \int_{-\infty}^{\infty} \mathrm{e}^{-(V-V_{50})^2/2\sigma^2}\, \mathrm{d}x \tag{8.7}$$

A plot of this function is included in Fig. 8.12. When plotted on the probability scale a straight line results as shown in Fig. 8.13. In this figure are plotted the cumulative frequency $P_{WS}$ of withstand voltage, the $P_{FO}$ of flashover voltage and the parameter $z$, explained below, versus the breakdown voltage of a 1-m rod gap under positive switching impulse voltage in atmospheric air. We note

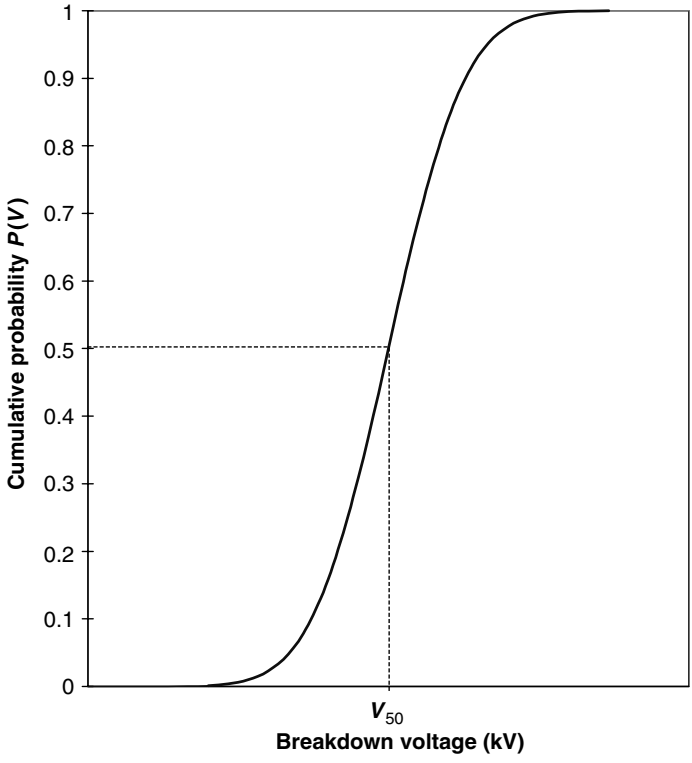


**Figure 8.12** *Gaussian cumulative distribution function*

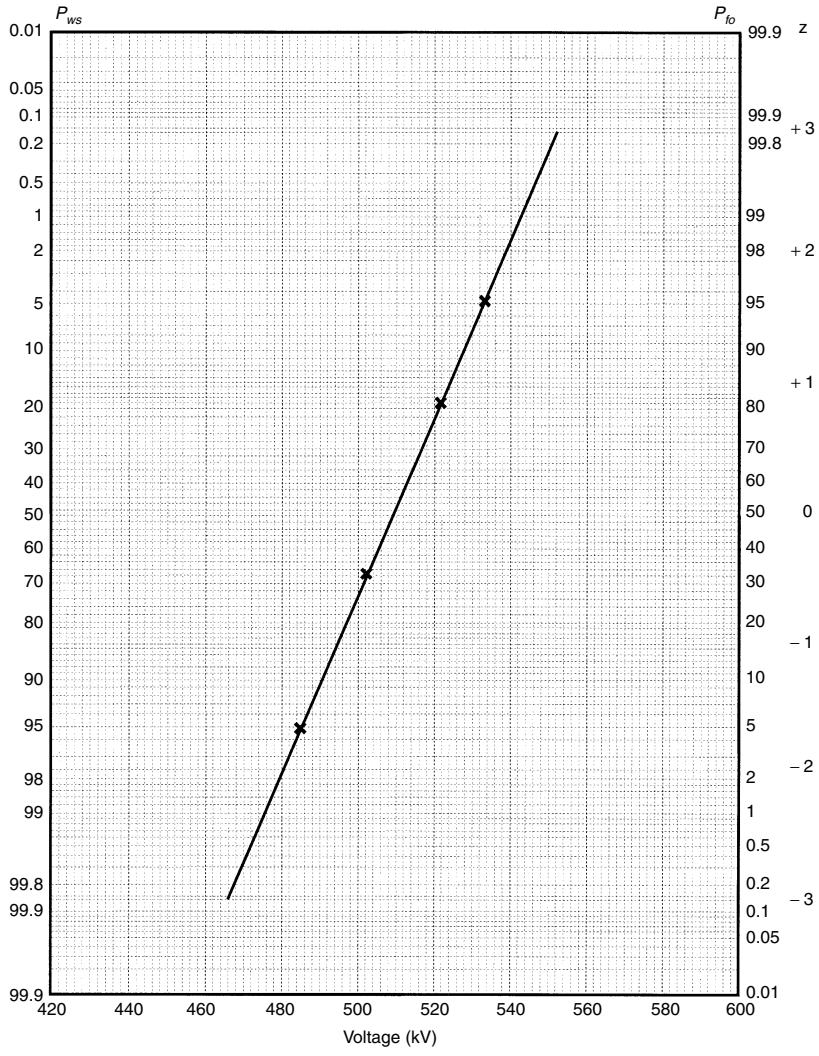


**Figure 8.13** *Breakdown voltage distribution plotted on probability scale*

that there are three vertical scales, two non-linear giving directly the $P_{WS}$ (l.h.s.), the $P_{FO}$ (r.h.s.) and further to the right a linear scale given in units of dimensionless deviation $z$. The parameter $z$ is convenient for analysis of normal distribution results. Equation (8.7) is rewritten in the form

$$P(\mathbf{z}) = \frac{1}{\sigma\sqrt{2\pi}} \int_{-\infty}^{z} \mathrm{e}^{-(z^2/2)}\, \mathrm{d}z \tag{8.8}$$

where

$$\mathbf{z} = \frac{V - V_{50}}{\sigma}$$

As noted earlier the distribution of flashover of the gap is characterized by two parameters:

(i) $V_{50}$, called the critical flashover (CFO),
(ii) $\sigma$, called the standard deviation.

Both can be read directly from the best fit line drawn through the experimentally determined points. Note, that CFO corresponds to $z = 0$ and $\sigma$ is given by the difference between two consecutive integers of $z$. In practice the voltage range over which the probability of flashover is distributed is

$$\text{CFO} \pm 3\sigma \tag{8.9}$$

- $(\text{CFO} - 3\sigma)$ is known as the statistical withstand voltage (SWV) and represents the point with flashover probability 0.13 per cent;
- $(\text{CFO} + 3\sigma)$ is known as the statistical flashover voltage (SFOV) and represents the point with flashover probability 99.87 per cent.

The SWV and SFOV are used in insulation coordination and will be discussed later. For a complete description of insulation parameters, the time to breakdown must also be considered. The times to breakdown are represented by

$$P(t) = \frac{1}{\sigma\sqrt{2\pi}} \int_0^t \mathrm{e}^{-(t-\bar{t})^2/2\sigma^2}\, \mathrm{d}t \tag{8.10}$$

where

$\bar{t}$ = mean time to breakdown,
$\sigma$ = standard deviation.

An example of the distribution of times to breakdown is included in Fig. 8.14.

In this example the range

$$\bar{t} \pm \sigma = \bar{t} \pm z$$

is shown by a straight line but not at the extremities. Nevertheless the method is often used to represent distribution of times to breakdown because of its simplicity.

Another frequently used distribution function for representing breakdown voltage probability is the Weibull function of the form:

$$P(V) = 1 - 0.5^{[1+((V-V_{50})^m/n\sigma)\ln 2]} \tag{8.11}$$

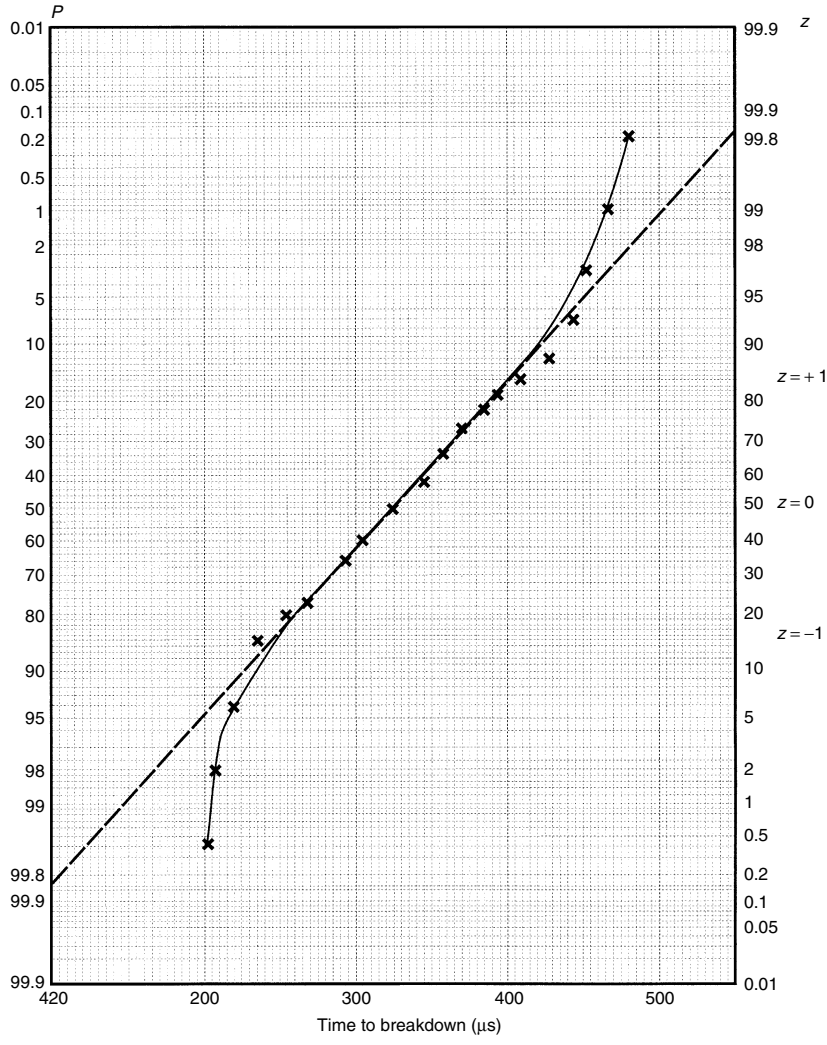


**Figure 8.14** *Distribution of times to breakdown*

where

$P(V)$ = the probability of flashover,
$V$ = the applied voltage,
$V_{50}$ = the applied voltage which gives 50 per cent probability flashover,
$\sigma$ = the standard deviation.

In the Weibull function $n$ is not known but it determines the voltage $V_{50} - n\sigma$ below which no flashover occurs, or $P(V) = 0$ for $V \leq V_{50} - n\sigma$. For air $n$

lies in the range $3 \leq n \leq 4$. The value 3 is usually used resulting in

$$m = \frac{\ln \dfrac{\ln 0.84}{\ln 0.5}}{\ln \dfrac{n-1}{n}} = 3.4 \tag{8.12}$$

The adaptation of the Weibull function to normal distribution using the above values for $n$ and $m$ gives $P(V) = 0.5$ for $V = V_{50}$ and $P(V) = 0.16$ for $V = V_{50} - \sigma$. Both the Gaussian and the Weibull functions give the same results in the range $0.01 \leq P(V) \leq 0.99$.

### 8.4.6 Errors and confidence in results

In the determination of a parameter two types of error are present:

(i) error associated with the statistical nature of the phenomena and the limited number of tests ($\varepsilon_S$),
(ii) error in the measurement ($\varepsilon_M$).

The statistical error is expressed by means of two confidence limits $C$ per cent. The total error is given by

$$\varepsilon_T = \sqrt{\varepsilon_M^2 + \varepsilon_S^2} \tag{8.13}$$

The various IEC recommendations specify the permissible measurement accuracy as 3 per cent. Hence, a statistical error of, say, 2 per cent will increase the total error by a factor of 1.2, while a statistical error of 1.5 per cent will increase the total error by 1.1.

The outcome of a test procedure and the analysis of the results is usually an average of a parameter $z$ with $C$ per cent confidence limits $z_A$ and $z_B$ (see Fig. 8.11). For a normal distribution the probability density of a function for a frequency of occurrence can be represented graphically in terms of area as shown in Fig. 8.11 $(1 - \alpha)$.

### 8.4.7 Laboratory test procedures

The test procedures applied to various types of insulation are described in national and international standards as already mentioned before.[12,13] Because the most frequently occurring overvoltages on electric systems and apparatus originate in lightning and switching overvoltages, most laboratory tests are conducted under standard lightning impulse voltages and switching surge voltages. Three general testing methods have been accepted:

1. Multi-level method.
2. Up and down method.
3. Extended up and down method.

### 1. Multi-level test method

In this method the procedure is:

- choose several test voltage levels,
- apply a pre-specified number of shots at each level ($n$),
- count the number ($x$) of breakdowns at each voltage level,
- plot $p(V)$ $(x_j/n)$ against $V$ (kV),
- draw a line of best fit on a probability scale,
- from the line determine $V_{50}$ at $z = 0$ or $P(V) = 50$ per cent,
- and $\sigma$ at $z = 1$ or $\sigma = V_{50\%} - V_{16\%}$

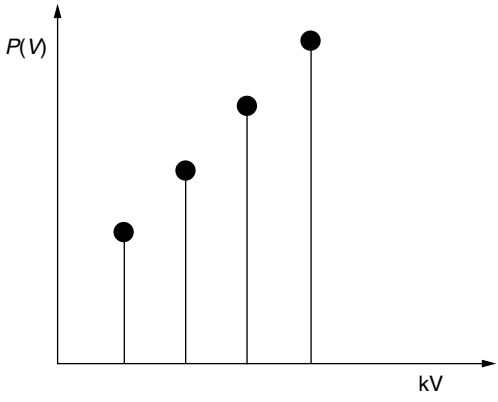


**Figure 8.15** *Probability of breakdown distribution using the multi-level method*

The recorded probability of breakdown, $x_j/n$, is the number which resulted in breakdown from the application of $n$ shots at voltage $V_j$. When $x_j/n$ is plotted against $V_j$ on a linear probability paper a straight line is obtained as shown in Fig. 8.15.

The advantage of this method is that it does not assume normality of distribution. The disadvantage is that it is time consuming, i.e. many shots are required.

This test method is generally preferred for research and live-line testing (typically 100 shots per level, with 6–10 levels).

### 2. Up and down method

In this method a starting voltage ($V_j$) close to the anticipated flashover value is selected. Then equally spaced voltage levels ($\Delta V$) above and below the starting

voltage are chosen. The first shot is applied at the voltage $V_j$. If breakdown occurs the next shot is applied at $V_j - \Delta V$. If the insulation withstands, the next voltage is applied at $V_j + \Delta V$. The sequential procedure of testing is illustrated in Fig. 8.16.

Figure 8.17 illustrates the sequence with nine shots applied to the insulation under test. The IEC Standard for establishing $V_{50}$ (50 per cent) withstand voltage requires a minimum $n = 20$ voltage applications for self-restoring

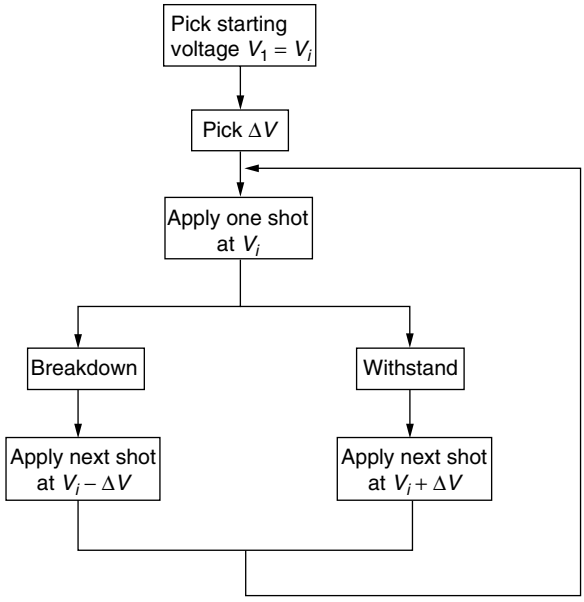


**Figure 8.16** *Schematics of the sequential up and down procedure*

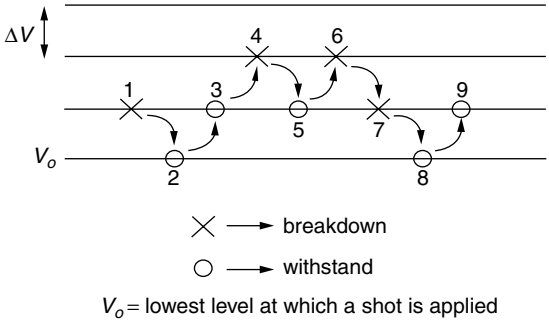


**Figure 8.17** *Example illustrating the application of nine shots in the sequential up and down method. X = breakdown; O = withstand*

insulation. To evaluate the $V_{10}$ (10 per cent) withstand voltage for self-restoring insulation with the up and down method with one impulse per group also requires a minimum of $n = 20$ applications.

In practice the points, expressing the probability of withstand, are plotted against the voltage $V_j$ on a probability scale graph as was shown in Fig. 8.13. The best straight line is then plotted using curve fitting techniques. The 50 per cent and 10 per cent discharge voltages are obtained directly from the graph. This method has the advantage that it requires relatively few shots and therefore is most frequently used by industry. The disadvantage is that it assumes normality and is not very accurate in determining $\sigma$. Alternatively, the $V_{10}$ can be obtained from the $V_{50}$ using the formula

$$V_{10} = V_{50}(1 - 1.3z) = V_{50} \cdot 0.96 \tag{8.14}$$

From the sequentially obtained readings (Fig. 8.17), the values of $V_{50}$ and $\sigma$ can be also calculated analytically as follows.

In the example chosen (Fig. 8.17): total number of shots $n = 9$, total number of breakdowns $n_b = 4$, total number of withstands $n_w = 5$, and lowest level at which a shot is applied $= V_0$.

In calculating $V_{50\%}$ and $\sigma$,

if $n_b > n_w$ then $n_i =$ number of withstands at level $j$

if $n_w > n_b$ then $n_j =$ number of breakdowns at level $j$

(always use the smaller of the two). The expressions are:

$$V_{50} = V_0 + \Delta V \left[\frac{A}{N} \pm \frac{1}{2}\right] \Rightarrow \begin{cases} n_i = n_{bi} \text{ use negative sign} \\ n_i = n_{wi} \text{ use positive sign} \end{cases} \tag{8.15}$$

$$\sigma = 1.62AV\left(\frac{NB - A^2}{N^2} + 0.029\right) \tag{8.16}$$

where

$$N = \sum_{i=0}^{k} n_{iw} \quad \text{or} \quad \sum_{i=0}^{k} n_{ib}$$

$$A = \sum_{i=0}^{k} i n_{iw} \quad \text{or} \quad \sum_{i=0}^{k} i n_{ib}$$

$$B = \sum_{i=0}^{k} i^2 n_{iw} \quad \text{or} \quad \sum_{i=0}^{k} i^2 n_{ib}$$

with $i$ referring to the voltage level, $n_{iw}$ to the number of withstands and $n_{ib}$ the number of breakdowns at that level.

### 3. The extended up and down method

This method is also used in testing self-restoring insulation. It can be used to determine discharge voltages corresponding to any probability $p$. A number of impulses are applied at a certain voltage level. If none causes discharge, the voltage is increased by a step $\Delta V$ and the impulses are applied until at least one causes breakdown, then the voltage is decreased. For an example of the extended up and down method procedure see Fig. 8.18.

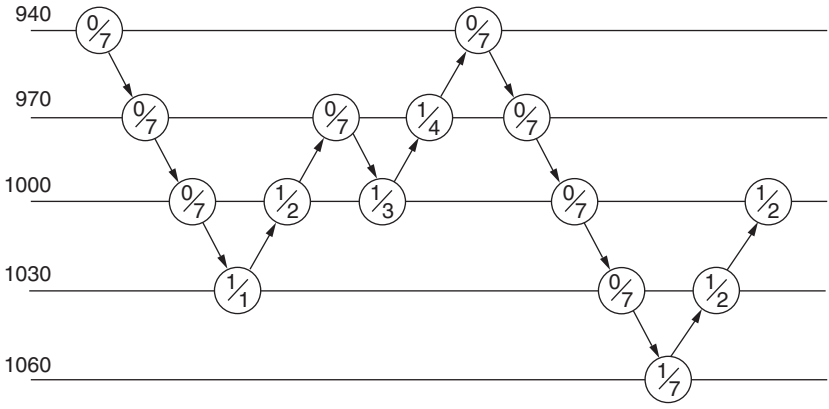


**Figure 8.18** *Example of the extended up and down method*

The number $n$ is determined such that a series of $n$ shots would have 50 per cent probability of giving at least one flashover. The 50 per cent probability of discharge is given by

$$0.5 = 1 - (1 - p)^n$$

or

$$n = 0.5 = \ln(1 - p) \tag{8.17}$$

from which $p$ becomes a discrete value. The value $n = 7$ impulses per voltage level is often used as it allows the determination of 10 per cent discharge voltage without the necessity to use $\sigma$. Substituting $n = 7$ into eqn (8.17) gives $p = 0.094$ or approximately 10 per cent.

The IEC switching withstand voltage is defined as 10 per cent withstand, hence the extended up and down method has an advantage. Other advantages include: discharge on test object is approximately 10 per cent the number of applied impulses rather than 50 per cent as applicable to the up and down

method. Also the highest voltage applied is about $V_{50}$ rather than $V_{50} + 2$. In the up and down method the $V_{10\%}$ may also be obtained from:

$$V_{10} = V_{50}\,(1 - 1.13z) = V_{50} \cdot 0.96 \tag{8.18}$$

In today's power systems for voltages up to 245 kV insulation tests are still limited to lightning impulses and the one-minute power frequency test. Above 300 kV, in addition to lightning impulses and the one-minute power frequency tests, tests include the use of switching impulse voltages.

### 8.4.8 Standard test procedures

#### 1. Proof of lightning impulse withstand level

For self-restoring insulation the test procedures commonly used for withstand establishment are:

(i) 15 impulses of rated voltage and of each polarity are applied, up to two disruptive discharges are permitted,
(ii) in the second procedure the 50 per cent flashover procedure using either the up and down or extended up and down technique as described earlier.

From the up and down method the withstand voltage is obtained using eqn (8.18). In tests on non-self-restoring insulation, three impulses are applied at the rated withstand voltage level of a specified polarity. The insulation is deemed to have withstood if no failure is observed.

#### 2. Testing with switching impulses

These tests apply for equipment at voltages above 300 kV. The testing procedure is similar to lightning impulses using 15 impulses. The tests are carried out in dry conditions while outdoor equipment is tested under positive switching impulses only. In some cases, when testing circuit isolators or circuit breakers which may experience combined voltage stress (power frequency and switching surge) biased tests using combined power frequency and surge voltages are used. The acceptable insulating capability requires 90 per cent withstand capability.

### 8.4.9 Testing with power frequency voltage

The standard practice requires the insulation to perform a one-minute test with power frequency at a voltage specified in the standards. For indoor equipment, the equipment is tested in dry conditions, while outdoor equipment is tested under prescribed rain conditions for which IEC prescribes a precipitation rate of 1–1.5 mm/min with resistivity of water.

### 8.4.10 Distribution of measured breakdown probabilities (confidence in measured P(V))

We apply at a level $V_i$, $n$ shots and obtain $x$ breakdowns. The outcome is breakdown or withstand, that is

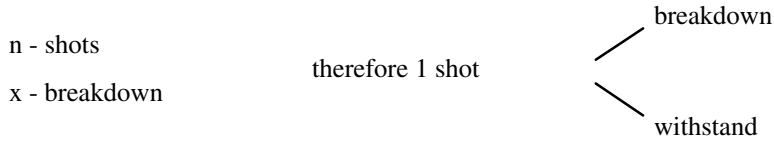


hence, the distribution of $P(V)$ is binomial around the expected value $x/n$. This distribution depends on $x$, $n$ and $q$ (the breakdown around which $P(x, n, \theta)$ is centre d) as shown in Fig. 8.19.

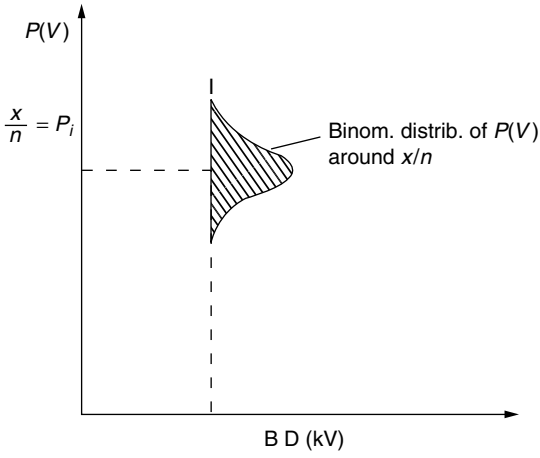


**Figure 8.19** *Binomial distribution of $P(V)$ around the expected value $x/n$*

$P_i$ is distributed around the value the point gives. For example, if we get: $V = 500\,\text{kV}$; P(FO) = 78 per cent, we do not really know that it is 78 per cent but we do know that it is distributed around 78 per cent.

The binomial distribution of $P$ around $x/n$ is given by

$$P(x, n, \theta) = \binom{n}{x} \theta^x (1-\theta)^{n-x}$$

where

$$\binom{n}{x} = \frac{n!}{x!(n-x)!}$$

$\theta$ = true value of the most likely outcome (value around which the distribution is centred).

We do not know $\theta$ but we can replace it with the expected value $x/n$ as was shown in Fig. 8.19.

Hence

$$P(x, n, \theta) = \binom{n}{x} \theta^x (1 - \theta) \tag{8.19}$$

with $x/n = 0.5$, $P(x)$ is symmetrical around $x/n$ but at extremities ($x/n = 1$ per cent and 99 per cent). $P(x)$ is skewed as seen in Figs 8.20(a) and (b).

To obtain these distributions, leave $x/n$ as the expected value and then vary $x$ to obtain the corresponding $P(x)$.

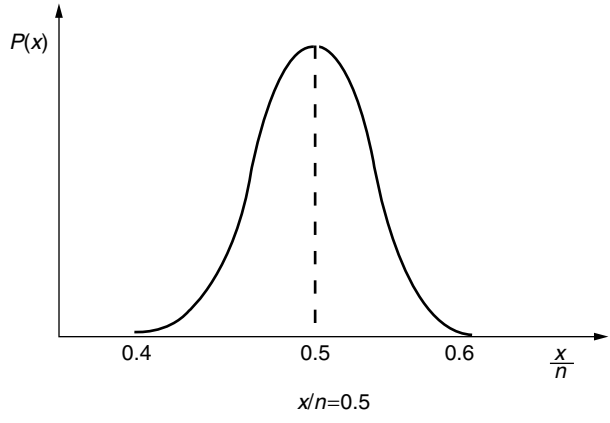


(a) $P(x)$ symmetric around

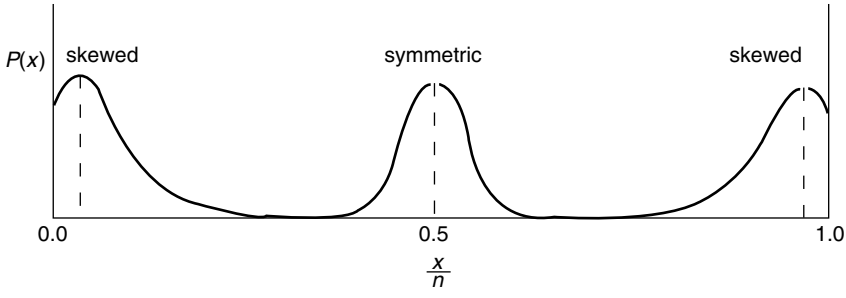


(b) Skewed

**Figure 8.20** *Relation between $P(x)$ and $x/n$: (a) Symmetric around $x/n = 0.5$. (b) Skewed*

### *Example*

$n = 5$; $x = 2$, therefore $x/n = 0.4$: find $P(x = 4)$, using eqn (8.19)

$$P(x = 4) = \frac{5!}{4!(5-4)!}(0.4)^4(1-0.4)^{(5-4)} = 7.7\%$$

Using the eqn (8.19) we find that as $n$ increases with $x/n$ being constant we have greater confidence in $P(x)$ as seen in Figs 8.21(a) and (b), while for small values of n the results are spread.

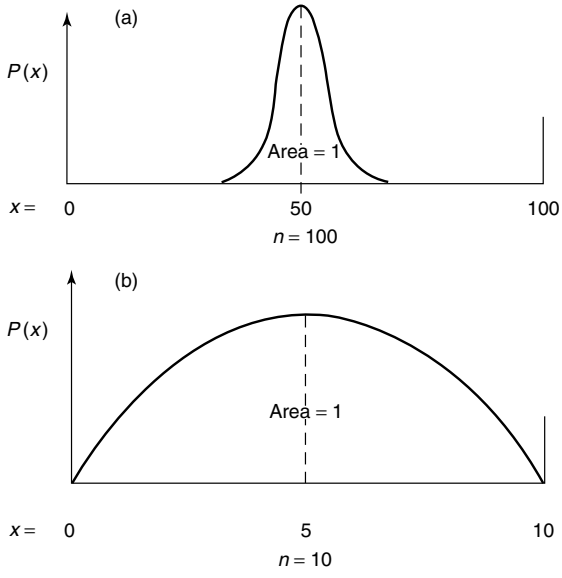


**Figure 8.21** *Effect of number of shots on $P(x)$ distribution: (a) $n = 100$; (b) $n = 10$*

### *8.4.11 Confidence intervals in breakdown probability (in measured values)*

The normalized value of the variable $x$ in the binomial distribution is

$$\frac{X - n\theta}{\sqrt{n\theta(1-\theta)}} \tag{8.20}$$

For a given level of confidence $1 - \alpha$ , where $\alpha$ is the level of significance as shown in Fig. 8.11, the confidence interval at a measured point is given by

$$-Z_{a/2} < \frac{x - n\theta}{\sqrt{n\theta(1-\theta)}} < +Z_{a/2} \tag{8.21}$$

The probability of breakdown with a confidence level $1-\alpha$ is given by

$$P(V) = \frac{x}{n} \pm Z_{a/2}\sqrt{\frac{\frac{x}{n}\left(1-\frac{x}{n}\right)}{n}} \tag{8.22}$$

Using this expression it can be shown on the linear probability scale that the confidence in the measured values of breakdown is at maximum at $x/n = 0.5$ and progressively decreases as the extreme values of breakdown probability are approached. $Z_{a/2}$ is obtained from tables of statistics or for convenience from the graph directly.

### *Example*

$n = 10$; $x = 5$ for a confidence level of 90 per cent

$$\alpha = 1 - 0.9 = 0.1$$

using statistical tables,[25] we obtain for

$$\frac{a}{2} = 0.05, \quad Z_{a/2} = 1.64$$

hence

$$P(V) = \tfrac{1}{2} \pm (1.64)\sqrt{\frac{\frac{1}{2}\left(\frac{1}{2}\right)}{10}}$$

The confidence limit at near $P(V) = 50$ per cent is much smaller than the confidence limit for $P(V)$ approaching 1 per cent or 99 per cent. The solution is a non-linear distribution of $n$, that is we need to take many shots near the limits and a few in the middle. Confidence expressed in terms of kV is more convenient than confidence in probability as shown in Fig. 8.22.

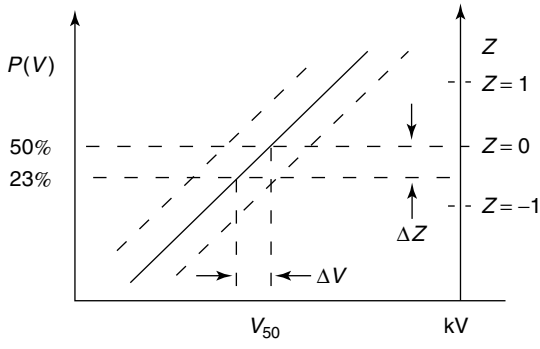


**Figure 8.22** *Confidence expressed in kV*

Using the same example as before

$23\% \leq P(V_{50}) \leq 77\%$

to determine $\Delta_z = z_1 - z_2$

$z_1$ is determined from the value of $P(0.50)$

$z_2$ is determined from the value of $P(0.23)$

from Fig. 8.22

for $F(z) = 50\% = 0.5,\ z_1 = 0.0$

for $F(z) = 23\% = -0.77,\ z_2 = -0.74$

therefore

$$\begin{aligned}\Delta z &= z_1 - z_2 \\ &= 0 - (-0.74) \\ &= 0.74\end{aligned}$$

the standard deviation $\sigma$ is the run from $z = 0$ to $z = 1$ therefore

$$\begin{aligned}\text{rise} &= \text{slope} \\ &= \Delta z/\Delta V \\ &= 1/\sigma\end{aligned}$$

and therefore $\Delta V = \Delta z\sigma$

Thus the confidence in $V$ is

$$\begin{aligned}V &= V \pm \Delta V \\ &= V \pm \Delta z\sigma \qquad (8.23)\end{aligned}$$

confidence in

$$V_{50} = V_{50} \pm (0.74)\sigma \qquad (8.24)$$

## 8.5 Weighting of the measured breakdown probabilities

Weights can be assigned to various data points to the measured breakdown probability and the number of impulses applied at each level.

### *8.5.1 Fitting of the best fit normal distribution*

On probability paper the normal distribution best characterizing the data points will appear as the best fit straight line. An example of this is shown in Fig. 8.23.

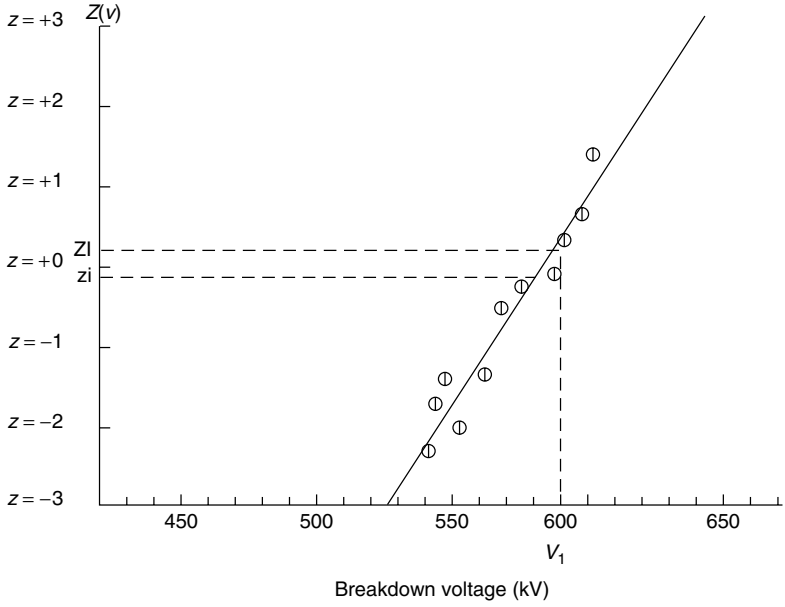


**Figure 8.23** *Best fit normal distribution drawn through measured flashover probability points*

In order to obtain this best fit straight line, it is necessary to minimize the deviation of the data points around the line. The root mean square deviation for the case shown in Fig. 8.23 is given by

$$\sqrt{\frac{1}{m}\sum_{i=1} w_i\,(z_i - \xi_i)^2} \tag{8.25}$$

where $x_i$ is the value of the measured breakdown probability on the probit scale at the voltage level $V_i$, $x_i$ is the probit scale value of the breakdown probability as given by the best fit straight line for the same voltage level, and $w_1$ is the weighting coefficient assigned to the measurement, $x_i$. The expression given in eqn (8.25) is in terms of the dimensionless deviation $z$. This can be rewritten using

$$z_i = \frac{V_i - V_{50}}{\sigma} \tag{8.26}$$

to obtain

$$\sqrt{\frac{1}{m}\sum_{i=1} w_i \left(\frac{V_i - V_{50}}{\sigma} - \xi_i\right)^2} \tag{8.27}$$

Minimizing this expression is equivalent to minimizing

$$\sum_{i=1} w_i \left( \frac{V_i - V_{50}}{\sigma} - \xi_i \right)^2 \tag{8.28}$$

The minimum value of the above expression occurs when the quantity

$$\sum_{i=1} w_i \, (V_i - V_{50} - \sigma \xi_i)^2 \tag{8.29}$$

is at its minimum. The best fit straight line which is in fact the normal distribution best representing the breakdown probability can now be obtained by setting

$$\frac{\partial}{\partial V_{50}} \sum_{i=1} w_i \, (V_i - V_{50} - \sigma \xi_i)^2 = 0 \tag{8.30}$$

and

$$\frac{\partial}{\partial^{\sigma}} \sum_{i=1} w_i \, (V_i - V_{50} - \sigma \xi_i)^2 = 0 \tag{8.31}$$

and solving for $V_{50}$ and $\sigma$. These values are found by carrying out the partial differentiation of eqns (8.30) and (8.31). This gives the following two simultaneous equations

$$\sum_{i=1} w_i \, v_i - \sum_{i=1} w_i V_{50} - \sigma \sum_{i=1} w_i \xi_i = 0 \tag{8.32}$$

and

$$\sum_{i=1} w_i V_i \xi_i - V_{50} \sum_{i=1} w_i \xi_i - \sigma \sum_{i=1} w_i \xi_i^2 = 0 \tag{8.33}$$

which can be solved to obtain

$$V_{50} = \frac{\sum_{i=1} w_i V_i - \sigma \sum_{i=1} w_i \xi_i}{\sum_{i=1} w_i} \tag{8.34}$$

and

$$\sigma = \frac{\sum_{i=1} w_i V_i \sum_{i=1} w_i \xi_i - \sum_{i=1} w_i \sum_{i=1} w_i V_i \xi_i}{\left( \sum_{i=1} w_i \xi_i \right)^2 - \sum_{i=1} w_i \sum_{i=1} w_i \xi_i^2} \tag{8.35}$$

Thus values for $V_{50}$ and $\sigma$ are obtained.

## 8.6 Insulation coordination

Insulation coordination is the correlation of insulation of electrical equipment with the characteristics of protective devices such that the insulation is protected from excessive overvoltages. In a substation, for example, the insulation of transformers, circuit breakers, bus supports, etc., should have insulation strength in excess of the voltage provided by protective devices.

Electric systems insulation designers have two options available to them: (i) choose insulation levels for components that would withstand all kinds of overvoltages, (ii) consider and devise protective devices that could be installed at the sensitive points in the system that would limit overvoltages there. The first alternative is unacceptable especially for e.h.v. and u.h.v. operating levels because of the excessive insulation required. Hence, there has been great incentive to develop and use protective devices. The actual relationship between the insulation levels and protective levels is a question of economics. Conventional methods of insulation coordination provide a margin of protection between electrical stress and electrical strength based on predicted maximum overvoltage and minimum strength, the maximum strength being allowed by the protective devices.

### *8.6.1 Insulation level*

'Insulation level' is defined by the values of test voltages which the insulation of equipment under test must be able to withstand.

In the earlier days of electric power, insulation levels commonly used were established on the basis of experience gained by utilities. As laboratory techniques improved, so that different laboratories were in closer agreement on test results, an international joint committee, the Nema-Nela Committee on Insulation Coordination, was formed and was charged with the task of establishing insulation strength of all classes of equipment and to establish levels for various voltage classification. In 1941 a detailed document[18] was published giving basic insulation levels for all equipment in operation at that time. The presented tests included standard impulse voltages and one-minute power frequency tests.

In today's systems for voltages up to 245 kV the tests are still limited to lightning impulses and one-minute power frequency tests, see section 8.3. Above 300 kV, in addition to lightning impulse and the one-minute power frequency tests, tests include the use of switching impulse voltages. Tables 8.2 and 8.3 list the standardized test voltages for $\leq$245 kV and above $\geq$300 kV respectively, suggested by IEC for testing equipment. These tables are based on a 1992 draft of the IEC document on insulation coordination.

**Table 8.2** *Standard insulation levels for Range I (1 kV < $U_m$ ≤ 245 kV) (From IEC document 28 CO 58, 1992, Insulation coordination Part 1: definitions, principles and rules)*

| *Highest voltage for equipment* $U_m$ *kV (r.m.s. value)* | *Standard power frequency short-duration withstand voltage kV (r.m.s. value)* | *Standard lightning impulse withstand voltage kV (peak value)* |
|---|---|---|
| 3.6 | 10 | 20 |
| | | 40 |
| 7.2 | 20 | 40 |
| | | 60 |
| 12 | 28 | 60 |
| | | 75 |
| | | 95 |
| 17.5 | 38 | 75 |
| | | 95 |
| 24 | 50 | 95 |
| | | 125 |
| | | 145 |
| 36 | 70 | 145 |
| | | 170 |
| 52 | 95 | 250 |
| 72.5 | 140 | 325 |
| 123 | (185) | 450 |
| | 230 | 550 |
| 145 | (185) | (450) |
| | 230 | 550 |
| | 275 | 650 |
| 170 | (230) | (550) |
| | 257 | 650 |
| | 325 | 750 |
| 245 | (275) | (650) |
| | (325) | (750) |
| | 360 | 850 |
| | 395 | 950 |
| | 460 | 1050 |

**Table 8.3** *Standard insulation levels for Range II ($U_m > 245\,kV$) (From IEC document 28 CO 58, 1992, Insulation coordination Part 1: definitions, principles and rules)*

| *Highest voltage for equipment $U_m$ kV (r.m.s. value)* | *Longitudinal insulation (+) kV (peak value)* | *Standard lightning impulse withstand voltage Phase-to-earth kV (peak value)* | *Phase-to-phase (ratio to the phase-to-earth peak value)* | *Standard lightning impulse withstand voltage kV (peak value)* |
|---|---|---|---|---|
| 300 | 750 | 750 | 1.50 | 850<br>950 |
| | 750 | 850 | 1.50 | 950<br>1050 |
| 362 | 850 | 850 | 1.50 | 950<br>1050 |
| | 850 | 950 | 1.50 | 1050<br>1175 |
| 420 | 850 | 850 | 1.60 | 1050<br>1175 |
| | 950 | 950 | 1.50 | 1175<br>1300 |
| | 950 | 1050 | 1.50 | 1300<br>1425 |
| 525 | 950 | 950 | 1.70 | 1175<br>1300 |
| | 950 | 1050 | 1.60 | 1300<br>1425 |
| | 950 | 1175 | 1.50 | 1425<br>1550 |
| 765 | 1175 | 1300 | 1.70 | 1675<br>1800 |
| | 1175 | 1425 | 1.70 | 1800<br>1950 |
| | 1175 | 1550 | 1.60 | 1950<br>2100 |

(+)Value of the Impulse component of the relevant combined test.
**Note**: The introduction of $U_m = 550\,kV$ (instead of 525 kV), 800 kV (instead of 765 kV), 1200 kV, of a value between 765 kV and the associated standard withstand voltages, are under consideration.

### 8.6.2 Statistical approach to insulation coordination

In the early days insulation levels for lightning surges were determined by evaluating the 50 per cent flashover values (BIL) for all insulations and providing a sufficiently high withstand level that all insulations would withstand. For those values a volt–time characteristic was constructed. Similarly the protection levels provided by protective devices were determined. The two volt–time characteristics are shown in Fig. 8.24. The upper curve represents the common BIL for all insulations present, while the lower represents the protective voltage level provided by the protective devices. The difference between the two curves provides the safety margin for the insulation system. Thus the

$$\text{Protection ratio} = \frac{\text{Max. voltage it permits}}{\text{Max. surge voltage equipment withstands}} \tag{8.36}$$

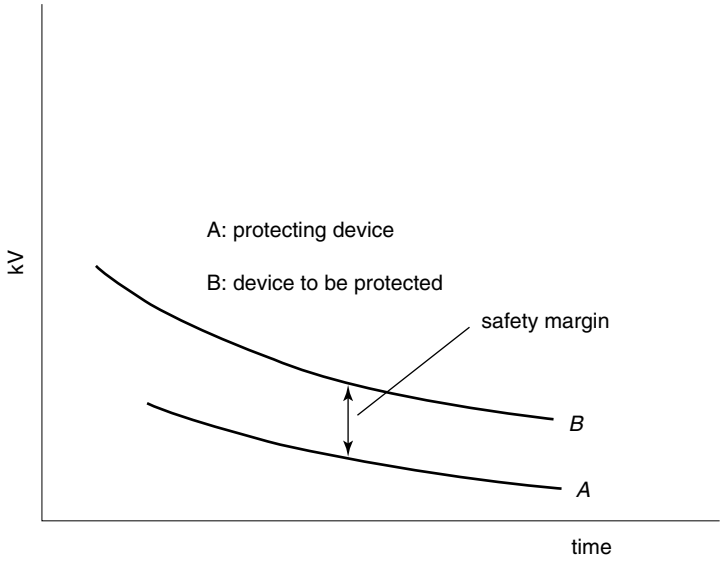


**Figure 8.24** *Coordination of BILs and protection levels (classical approach)*

This approach is difficult to apply at e.h.v. and u.h.v. levels, particularly for external insulations.

Present-day practices of insulation coordination rely on a statistical approach which relates directly the electrical stress and the electrical strength.[11] This approach requires a knowledge of the distribution of both the anticipated stresses and the electrical strengths.

The statistical nature of overvoltages, in particular switching overvoltages, makes it necessary to compute a large number of overvoltages in order to determine with some degree of confidence the statistical overvoltages on a system. The e.h.v. and u.h.v. systems employ a number of non-linear elements, but with today's availability of digital computers the distribution of overvoltages can be calculated. A more practical approach to determine the required probability distributions of a system's overvoltages employs a comprehensive systems simulator, the older types using analogue units, while the newer employ real time digital simulators (RTDS).[24]

For the purpose of coordinating the electrical stresses with electrical strengths it is convenient to represent the overvoltage distribution in the form of probability density function (Gaussian distribution curve as shown in Fig. 8.11) and the insulation breakdown probability by the cumulative distribution function (shown in Fig. 8.12). The knowledge of these distributions enables us to determine the 'risk of failure'. As an example, let us consider a case of a spark gap for which the two characteristics in Figs 8.11 and 8.12 apply and plot these as shown in Fig. 8.25.

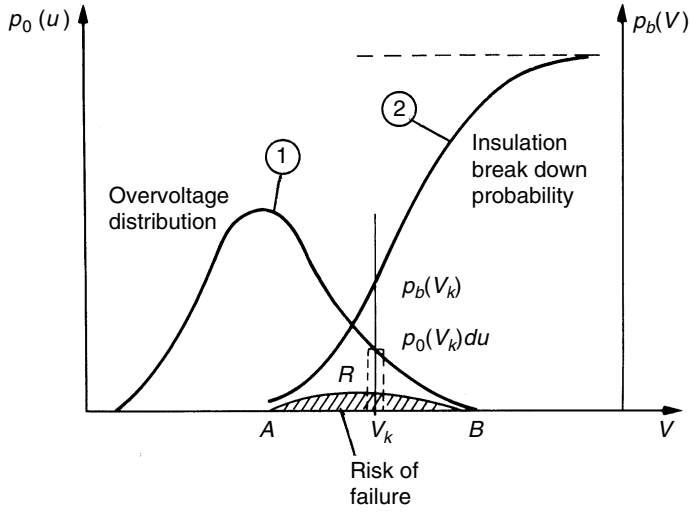


**Figure 8.25** *Method of describing the risk of failure. 1. Overvoltage distribution–Gaussian function. 2. Insulation breakdown probability–cumulative distribution)*

If $V_a$ is the average value of overvoltage, $V_k$ is the $k$th value of overvoltage, the probability of occurrence of overvoltage is $p_0(V_k)\,\mathrm{d}u$, whereas the probability of breakdown is $P_b(V_k)$ or the probability that the gap will break down at an overvoltage $V_k$ is $P_b(V_k)p_0(V_k)\,\mathrm{d}u$. For the total voltage

range we obtain for the total probability of failure or 'risk of failure'

$$R = \int_0^\infty P_b(V_k)\, p_0(V_k)\, \mathrm{d}u. \tag{8.37}$$

The risk of failure will thus be given by the shaded area under the curve $R$.

In engineering practice it would become uneconomical to use the complete distribution functions for the occurrence of overvoltage and for the withstand of insulation and a compromise solution is accepted as shown in Figs 8.26(a) and (b) for guidance. Curve (a) represents probability of occurrence of overvoltages of such amplitude ($V_s$) that only 2 per cent (shaded area) has a chance to cause breakdown. $V_S$ is known as the 'statistical overvoltage'. In Fig. 8.26(b) the voltage $V_w$ is so low that in 90 per cent of applied impulses, breakdown does not occur and such voltage is known as the 'statistical withstand voltage' $V_w$.

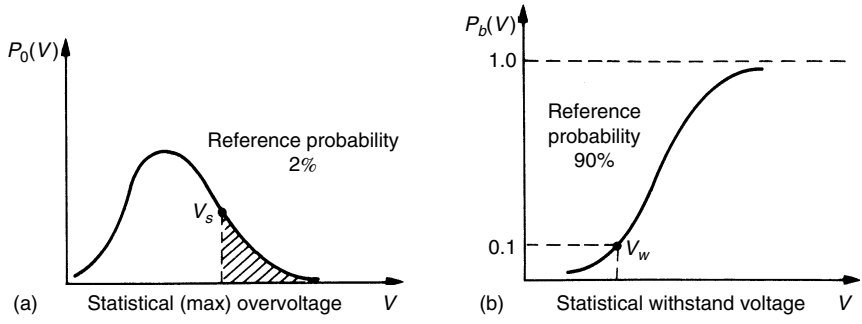


**Figure 8.26** *Reference probabilities for overvoltage and for insulation withstand strength*

In addition to the parameters statistical overvoltage '$V_S$' and the statistical withstand voltage '$V_W$' we may introduce the concept of statistical safety factor $\gamma$. This parameter becomes readily understood by inspecting Figs 8.27(a) to (c) in which the functions $P_b(V)$ and $p_0(V_k)$ are plotted for three different cases of insulation strength but keeping the distribution of overvoltage occurrence the same. The density function $p_0(V_k)$ is the same in (a) to (c) and the cumulative function giving the yet undetermined withstand voltage is gradually shifted along the $V$-axis towards high values of $V$. This corresponds to increasing the insulation strength by either using thicker insulation or material of higher insulation strength. As a result of the relative shift of the two curves [$P_b(V)$ and $p_0(V_k)$] the ratio of the values $V_w/V_s$ will vary. This ratio is known as the statistical safety factor or

$$\frac{V_w}{V_s} = \gamma \tag{8.37}$$

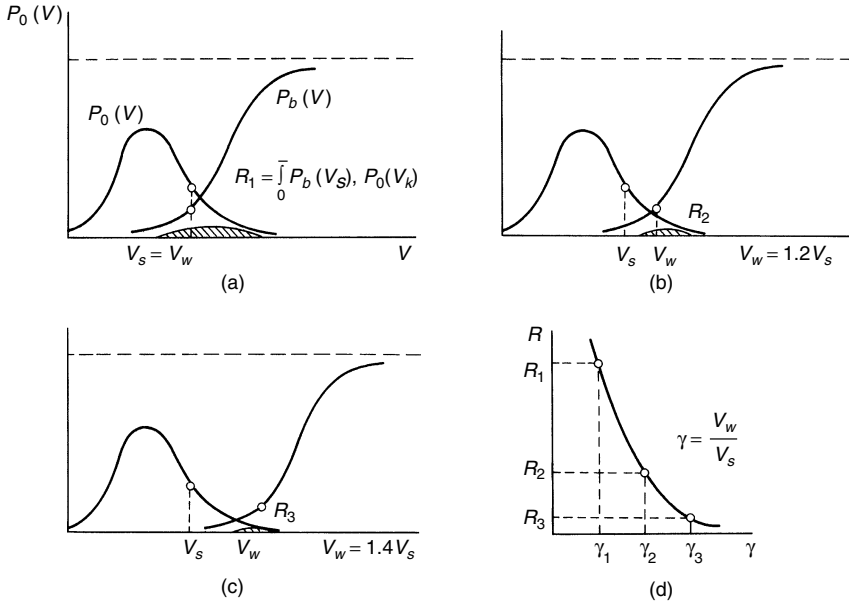


**Figure 8.27** *The statistical safety factor and its relation to the risk of failure (R)*

In the same figure (d) is plotted the relation of this parameter to the 'risk of failure'. It is clear that increasing the statistical safety factor ($\gamma$) will reduce the risk of failure ($R$), but at the same time will cause an increase in insulation costs. The above treatment applies to self-restoring insulations. In the case of non-self-restoring insulations the electrical withstand is expressed in terms of actual breakdown values. The statistical approach to insulation, presented here, leads to withstand voltages (i.e. probability of breakdown is very small), thus giving us a method for establishing the 'insulation level'.

### *8.6.3 Correlation between insulation and protection levels*

The 'protection level' provided by (say) arresters is established in a similar manner to the 'insulation level'; the basic difference is that the insulation of protective devices (arresters) must not withstand the applied voltage. The concept of correlation between insulation and protection levels can be readily understood by considering a simple example of an insulator string being protected by a spark gap, the spark gap (of lower breakdown strength) protecting the insulator string. Let us assume that both gaps are subjected to the same overvoltage represented by the probability density function $p_0(V)$, Fig. 8.28. The probability distribution curves for the spark gap and the insulator string are presented by $P_g(V)$ and $P_i(V)$ respectively in Fig. 8.28.

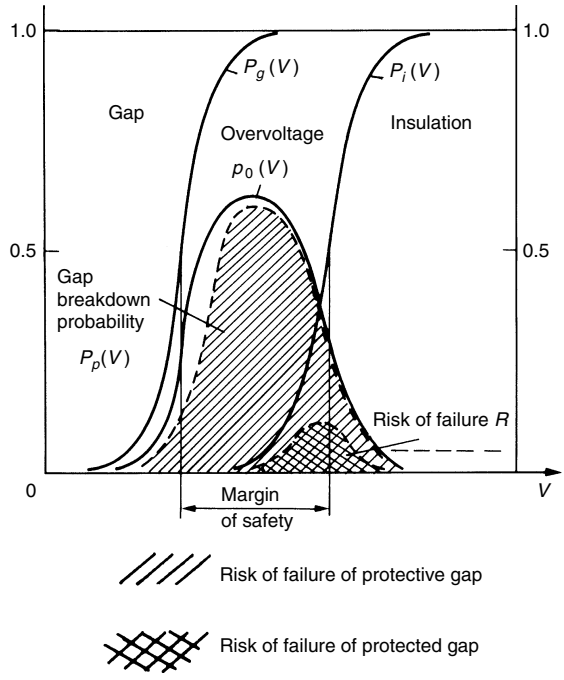


**Figure 8.28** *Distribution functions of breakdown voltages for protective gap and protected insulation both subjected to an overvoltage* $p_0(V)$

The statistical electrical withstand strength of the insulator string is given by a curve identical to Fig. 8.26. The probability of breakdown of this insulation remains in the area $R$ which gives 'risk of failure'. Since the string is protected by a spark gap of withstand probability $P_g(V)$, the probability that the gap will operate (its risk of failure) is obtained from integrating the product $P_g(V)p_0(V)\,\mathrm{d}V$. In Fig. 8.28 this probability is denoted (qualitatively) by $P_P(V)$. As is seen the probability is much higher than the probability of insulation damage or failure $R$. In the same figure is shown the traditional margin of safety corresponding to the voltage difference between the 50 per cent flashover values of the protecting gap and the protected gap.

For overvoltages of the highest amplitude (extreme right of Fig. 8.28) the probability curves of insulation failure and that of protective spark gap breakdown overlap. In reality such cases will not arise. Figure 8.28 is simplified in that it contains information pertaining to the amplitude of the overvoltage, and ignores the effect of time of voltage application on the breakdown of both the protective gap and the insulation. In practice, the protective gap will in general break down before the insulation and will cause a reduction (to a safe limit) in overvoltage reaching the protected insulation.

## 8.7 Modern power systems protection devices

### *8.7.1 MOA – metal oxide arresters*

The development of MOA (metal oxide arresters) represented a breakthrough in overvoltage protection devices. It became possible to design arresters without using gaps which were indispensable in the conventional lightning arresters, which utilized non-linear resistors made of silicon Carbide (SiC) and spark gaps. Figure 8.29 shows a block diagram of the valve arrangements in the two types of arrester.

In (a) the elements and the spark gaps are connected in series. In (b) the elements are stacked on top of each other without the need for spark gaps.

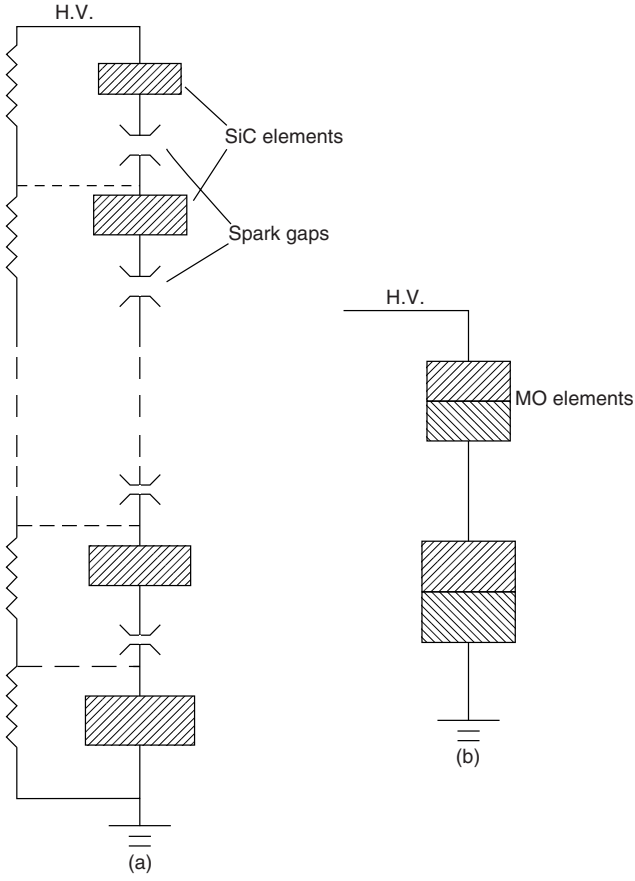


**Figure 8.29** *Block diagram of valve arrangements in (a) SiC, (b) MOA*

An ideal lightning arrester should: (i) conduct electric current at a certain voltage above the rated voltage; (ii) hold the voltage with little change for the duration of overvoltage; and (iii) substantially cease conduction at very nearly the same voltage at which conduction started.[25] In Fig. 8.29(a) the three functions are performed by the combination of the series spark gaps and the SiC elements. In the (b) case the metal oxide valve elements perform all three functions because of their superior non-linear resistivity.

The volt–current characteristics for the two types of arresters can be represented by the following equations:

$$\text{For SiC valves: } I = kV^a \quad \text{where } a = 4\text{–}6 \tag{8.38}$$

$$\text{For ZnO valves: } I = kV^b \quad \text{where } k = \text{const}, \; b = 25\text{–}30 \tag{8.39}$$

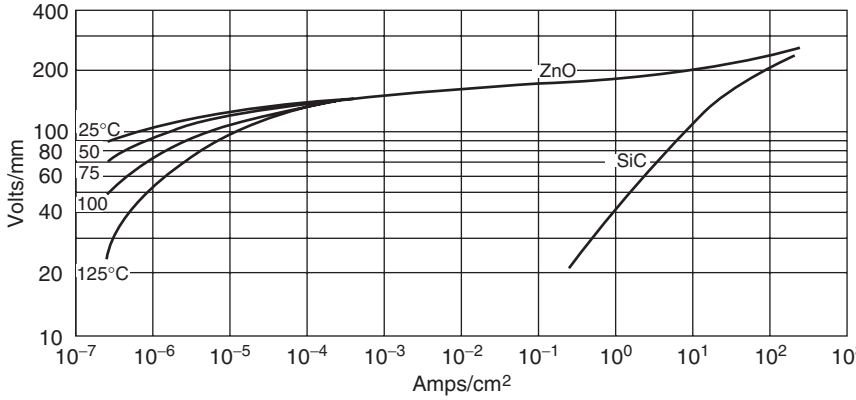


**Figure 8.30** *Normalized volt–ampere characteristic of zinc oxide and silicon carbide valve elements*

Typical volt–current characteristics for the valve elements used in the two types of arresters are plotted in Fig. 8.30. The metal oxide varistors, which consist of compacted and sintered granules of zinc oxide with a small amount of other carefully selected metal oxide additives ($Bi_2O_3$, MnO, $Cr_2O_3$, $Sb_2O_3$) to improve the V–I non-linearity, were first introduced in the electronics industry in 1968 by Matsushita Electric Industrial Co. in Japan. The ZnO grains have a low resistivity, while the additives (oxides) which form the boundaries between the grains provide high resistance. The two are strongly bonded when sintered at high temperature. Figure 8.31 shows the microstructure of a metal oxide varistor.

Subsequently these were developed for use as a substitute for SiC valve blocks in surge arresters by General Electric Co.[26] From Fig. 8.30 it can be seen that for a change in current from $10^{-3}$ to $10^2$ A/cm$^2$, the voltage increase

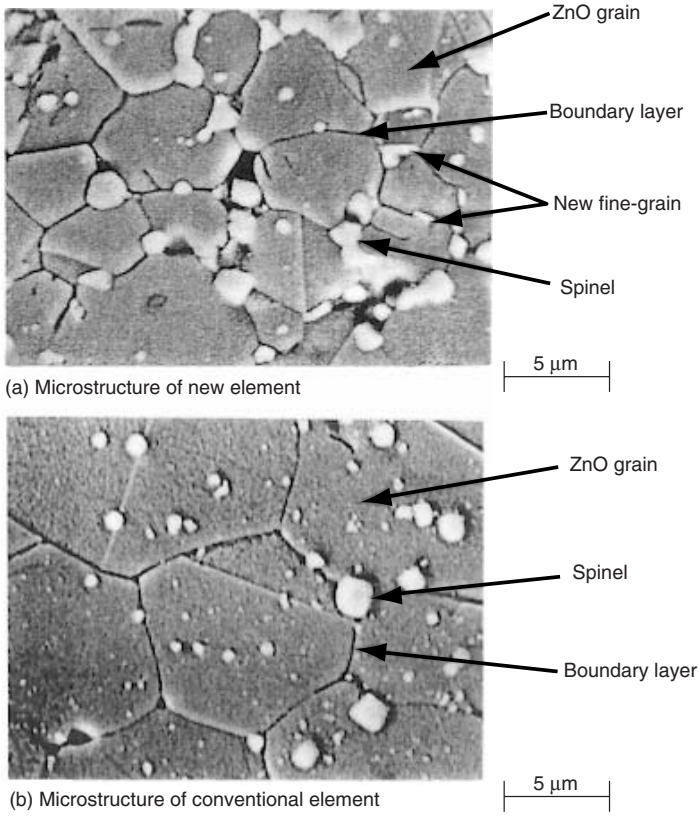


**Figure 8.31** *Cross-section, showing the microstructure of ZnO elements. (a) Latest type (advanced). (b) Older conventional type (courtesy of Mitsubishi Elec. Co.)*

for ZnO is only 56 per cent.[25] With such a high degree of non-linearity it is entirely feasible to use these elements without series gaps in an arrester with a current of only tens of μA at operating voltage.

The elements are manufactured in the form of discs of several sizes. The disc voltage rating has been increasing with the improvement in the manufacturing technology and the microstructure composition, e.g. Fig. 8.32 compares the $V-I$ characteristics of an older type ZnO element with that of a new type, both developed by Mitsubishi.[27]

It is noted that the voltage rating per unit valve has been approximately doubled. For higher voltage and current ratings the discs are arranged in series and in parallel. Figure 8.33 shows a schematic structure of a three-column arrangement of the arrester valves in an advanced MOA compact structure manufactured by Mitsubishi.[27]

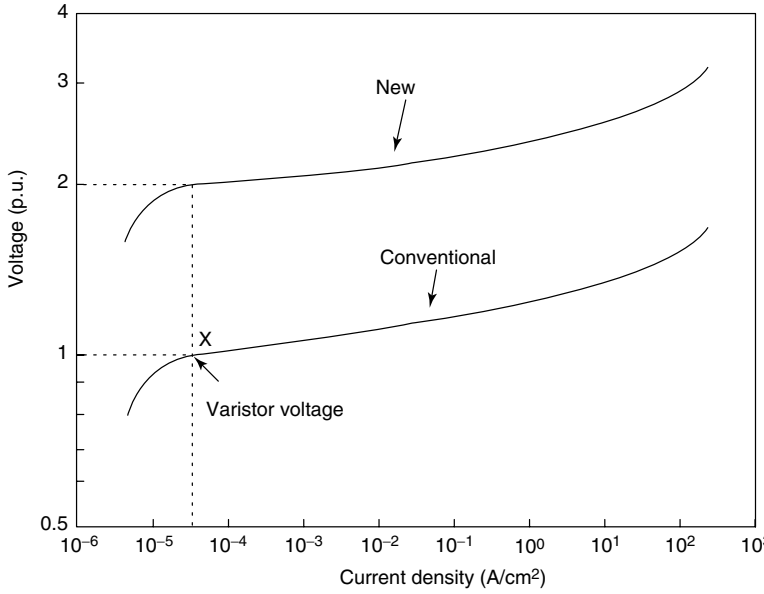


**Figure 8.32** *Comparison of volt–current characteristics of (a) advanced MOA with (b) that of an older type MOA (courtesy of Mitsubishi Co.)*

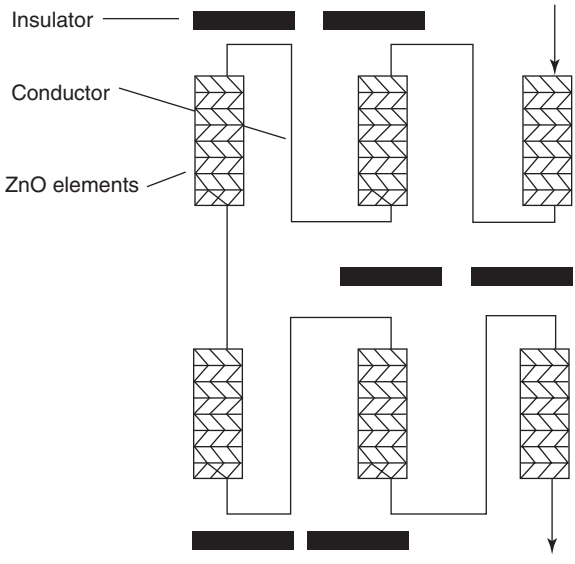


**Figure 8.33** *Schematic structure of a three column series arrangement of elements in advanced MOAs*

In Fig. 8.34 is shown part of an assembled advanced 500 kV MOA. The percentages indicate the reduction in size by replacing the older type MOA with the advanced MOA elements whose $V-I$ characteristics are shown in Fig. 8.32.

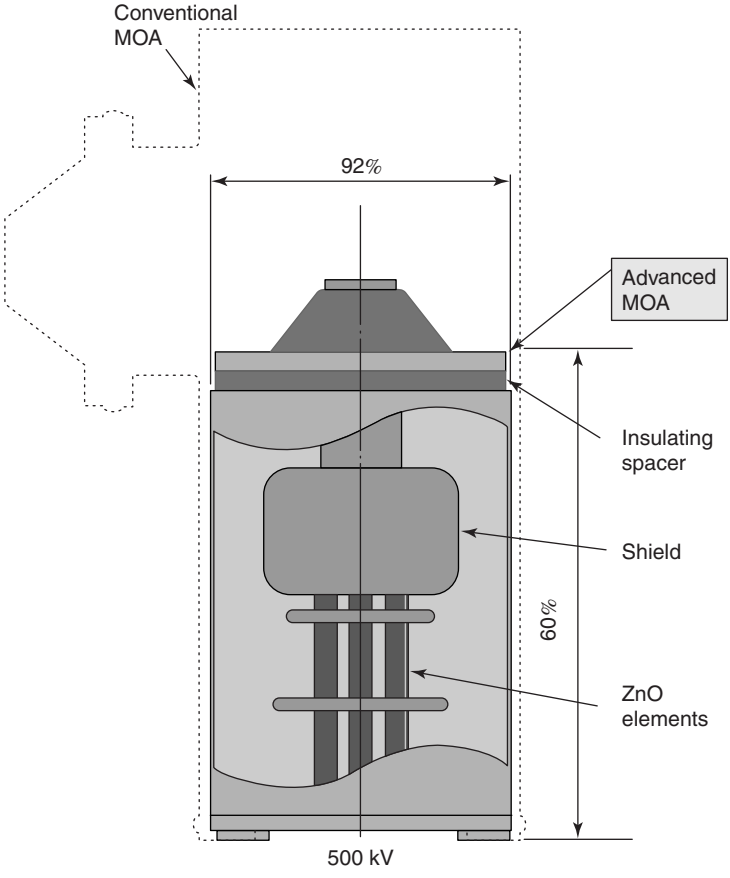


**Figure 8.34** *Part of an assembled 500 kV MOA Arrester. (courtesy of Mitsubishi Co.)*

In this construction the individual surge arresters are interconnected by means of corona-free stress distributors. The modular design and the lightweight construction allow easy on-site erection and in the event of any units failing the individual unit may be readily replaced.

The advantages of the polymeric-housed arresters over their porcelain-housed equivalents are several and include:

- No risk to personnel or adjacent equipment during fault current operation.
- Simple light modular assembly – no need for lifting equipment.

- Simple installation.
- High-strength construction eliminates accidental damage during transport.
- The use of EPDM and/or silicon rubber reduces pollution flashover problems.

Thus the introduction of ZnO arresters and their general acceptance by utilities since late 1980s, and in 1990s in protecting high voltage substations, has greatly reduced power systems protection problems.

In the earlier construction the valve elements were mounted within a ceramic housing. The metal oxide elements were surrounded by a gaseous medium and the end fittings were generally sealed with rubber O-rings. With time in service, especially in hostile environments, the seals tended to deterio-

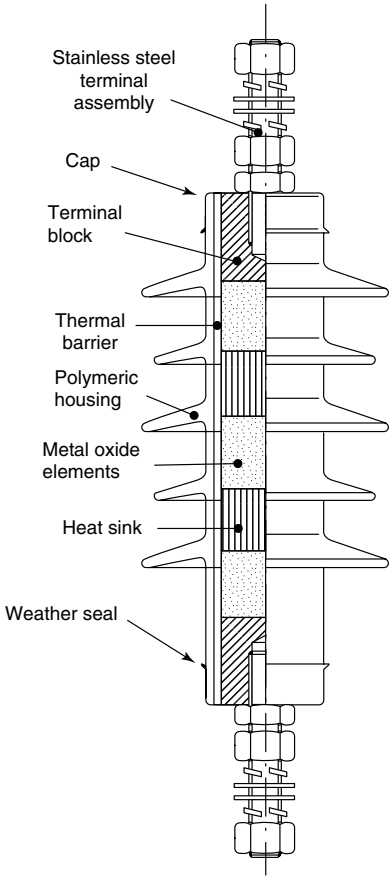


**Figure 8.35** *Cross-section of a polymer-housed arrester (courtesy of Bowthorpe EMP)*

rate allowing the ingress of moisture. In the 1980s polymeric-housed surge arresters were developed. Bowthorpe EMP (UK)[28] manufactures a complete range of polymeric-housed arresters extending from distribution to heavy duty station arresters for voltages up to 400 kV. In their design the surface of the metal oxide elements column is bonded homogeneously with glass fibre reinforced resin. This construction is void free, gives the unit a high mechanical strength, and provides a uniform dielectric at the surface of the metal oxide column. The housing material is a polymer (EPDM)–Ethylene propylene diene monomer–which is a hydrocarbon rubber, resistant to tracking and is particularly suitable for application in regions where pollution causes a problem. A cross-section detailing the major features of a polymeric-housed arrester is given in Fig. 8.35.

The ZnO elements are separated by aluminium blocks which serve as heat sinks. To achieve higher voltages and higher current ratings a modular construction with the individual units mounted in series–parallel arrangement is shown in Fig. 8.36.

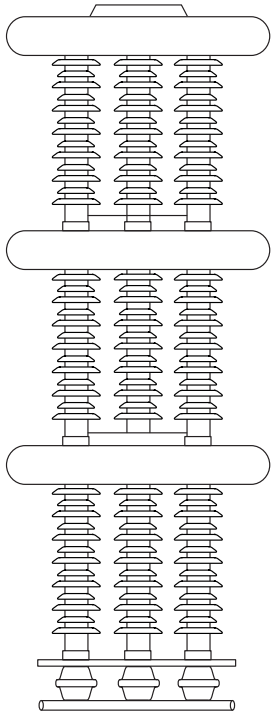

**Figure 8.36** *Construction of a series–parallel polymeric-housed arrester. (courtesy of Bowthorpe EMP)*